Biomaterials Advances 152 (2023) 213516

Contents lists available at ScienceDirect

Biomaterials Advances

journal homepage: www.journals.elsevier.com/materials-science-and-engineering-c

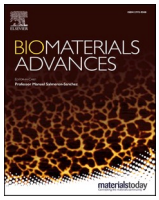

Mechanical activation of lung epithelial cells through the ion channel Piezo1 activates the metalloproteinases ADAM10 and ADAM17 and promotes growth factor and adhesion molecule release

Caroline Grannemann [a], Alessa Pabst [a], Annika Honert [a], Jana Schieren [b], Christian Martin [c], Sophia Hank [c], Svenja Böll [c], Katharina Bläsius [a], Stefan Düsterhöft [a], Holger Jahr [d], Rudolf Merkel [e], Rudolf Leube [b], Aaron Babendreyer [a,*,1], Andreas Ludwig [a,1]

[a] Institute of Molecular Pharmacology, RWTH Aachen University, Aachen, Germany
[b] Institute of Molecular and Cellular Anatomy, RWTH Aachen University, Aachen, Germany
[c] Institute of Pharmacology and Toxicology, RWTH Aachen University, Aachen, Germany
[d] Institute of Anatomy and Cell Biology, RWTH Aachen University, Aachen, Germany
[e] Institute of Biological Information Processing 2, Mechanobiology, Research Centre Juelich, Juelich, Germany

ARTICLE INFO

Keywords:
Mechanotransduction
Stretch
Epithelial lung cells
Ion channel
Metalloproteinase
Shedding
Cell junctions

ABSTRACT

In the lung, pulmonary epithelial cells undergo mechanical stretching during ventilation. The associated cellular mechanoresponse is still poorly understood at the molecular level. Here, we demonstrate that activation of the mechanosensitive cation channel Piezo1 in a human epithelial cell line (H441) and in primary human lung epithelial cells induces the proteolytic activity of the metalloproteinases ADAM10 and ADAM17 at the plasma membrane. These ADAMs are known to convert cell surface expressed proteins into soluble and thereby play major roles in proliferation, barrier regulation and inflammation. We observed that chemical activation of Piezo1 promotes cleavage of substrates that are specific for either ADAM10 or ADAM17. Activation of Piezo1 also induced the synthesis and ADAM10/17-dependent release of the growth factor amphiregulin (AREG). In addition, junctional adhesion molecule A (JAM-A) was shed in an ADAM10/17-dependent manner resulting in a reduction of cell contacts. Stretching experiments combined with Piezo1 knockdown further demonstrated that mechanical activation promotes shedding via Piezo1. Most importantly, high pressure ventilation of murine lungs increased AREG and JAM-A release into the alveolar space, which was reduced by a Piezo1 inhibitor. Our study provides a novel link between stretch-induced Piezo1 activation and the activation of ADAM10 and ADAM17 in lung epithelium. This may help to understand acute respiratory distress syndrome (ARDS) which is induced by ventilation stress and goes along with perturbed epithelial permeability and release of growth factors.

1. Introduction

Sensing and reacting to mechanical forces is an essential cellular response. It allows organisms to adapt to their mechanical environment. In vertebrates, the alveolar interface in the lung is exposed to mechanical forces as cells are stretched during respiration [1,2].

Mechanical forces can act from the outside of a cell to the inside and vice versa. This causes tension within the cell membrane and the submembranous actin cortex. The tension is sensed by the mechanosensitive ion channels Piezo1 and 2 that have recently received particularly high attention in research [3–6]. While Piezo2 is more relevant in neuronal cells, Piezo1 appears to be the predominant variant in many other cell types, such as endothelial, epithelial or immune cells [5]. Mechanical activation leads to opening of the channel and cation influx, which in turn leads to membrane depolarization due to sodium influx and several signalling events dependent on the influx of calcium. In this way, Piezo1 regulates physiological and pathological responses such as vascular development [7,8], blood pressure regulation [9], red blood cell volume regulation [10] and immune cell migration [11]. Piezo1 is also critically involved in epithelial homeostasis [12], ventilator-

* Corresponding author at: Institute of Molecular Pharmacology, RWTH Aachen University, Pauwelsstr. 30, 52074 Aachen, Germany.
E-mail address: ababendreyer@ukaachen.de (A. Babendreyer).
[1] Equal contribution.

https://doi.org/10.1016/j.bioadv.2023.213516
Received 22 December 2022; Received in revised form 25 April 2023; Accepted 9 June 2023
Available online 12 June 2023

induced lung injury [13] and regulation of surfactant production [14]. Furthermore, it has been described that mechanical stretch triggers rapid epithelial cell division via Piezo1 [15]. In vitro research on Piezo1 has been facilitated by the small molecule Yoda1 (2-[5-[[(2,6-dichlorophenyl)methyl]thio]-1,3,4-thiadiazol-2-yl]pyrazine), which activates Piezo1 but not Piezo2 [16], and the Piezo1 inhibitor salvianolic acid B (SalB) [17].

Piezo1-mediated cell signalling occurs at multiple levels and can result in transcriptional responses and posttranslational effects on proteins. Limited proteolysis is a critical posttranslational modification controlling effector functions of proteins. On the cell surface, proteolytically active members of the a disintegrin and metalloproteinase (ADAM) family control the function of cytokines, adhesion molecules, receptors and growth factors. ADAM10 and the closely related proteinase ADAM17 are the two best-studied members of the ADAM proteinase family. They cleave several types of surface molecules at an extracellular site proximal to the cell membrane resulting in the release of a soluble ectodomain [18,19]. This process has been termed shedding. Important substrates for ADAM10 are Notch, cadherins and the growth factor betacellulin [20]. The related proteinase ADAM17 is well known to cleave the proinflammatory cytokine TNF, but also contributes to the shedding of many other substrates including the growth factor amphiregulin (AREG) and the junctional adhesion molecule A (JAM-A) [20–22]. Due to these cleavage events, both proteinases are critically implicated in development, inflammatory responses and malignant diseases.

Since ADAM10 and ADAM17 are essential regulators of critical surface proteins, their activity is tightly controlled. This can occur at multiple levels involving gene induction, intracellular protein maturation, trafficking to the surface, conformational changes, lysosomal degradation or inhibitor interaction. Several posttranslational pathways promote the rapid increase in ADAM10 or ADAM17 activity [19,23]. Stimulation with the ionophore ionomycin (Iono) predominantly activates ADAM10 while stimulation with the protein kinase C (PKC) activator phorbol 12-myristate 13-acetate (PMA) preferentially enhances ADAM17 activity [24,25]. Besides these chemical activators, also physiological stimuli have been identified including ligands for G-protein-coupled receptors, toll-like receptors or ion channels. Signalling of endothelial cell expressed Piezo1 has been found to activate ADAM10 in response to shear stress [26]. So far, functional consequences of this activation have only been reported for endothelial cell expressed Notch1, which is cleaved by ADAM10 and then regulates transcription via its cell associated cleavage fragment [26].

In the present study, we provide novel evidence linking the stretch-induced activation of lung epithelial cells via Piezo1 to the activation of both metalloproteinases ADAM10 and ADAM17. Our investigations include several lines of evidence using the cultured alveolar epithelial cell line (H441), primary human lung epithelial cells and a murine ex vivo model in which the role of Piezo1 was studied by mechanical or chemical activation, inhibition or knockdown. We found that Piezo1-mediated cell activation results in ADAM10- and ADAM17-dependent release of the epithelial growth factor AREG and the junctional adhesion molecule JAM-A in vitro and ex vivo. The identified Piezo1/ADAM10/17 axis may contribute to epithelial permeability regulation via disassembly of cell junctions as well as to repair functions via release of epithelial growth factors.

2. Methods

2.1. Materials

Phorbol-12-myristat-13-acetat (PMA) and ionomycin (Iono) were purchased from Sigma-Aldrich (Steinheim, DE). TNF-alpha-Proteinase Inhibitor 1 (TAPI1) and GSK1016790A (GSK) was from Selleckchem (Houston, USA). GI254023X (GI) was from GlaxoSmithKline (Brentford, UK). Yoda1 and BIM2 was from Tocris (Minneapolis, USA). Salvianolic acid B (SalB) was from MedChemExpress (Monmouth Junction, USA). For antibodies used in this study, see the respective method sections.

2.2. Murine and human tissue

Ex vivo experiments with isolated perfused murine lungs of female C57BL/6 N mice (20–25 g) were approved by the Institute for Laboratory Animal Science and Experimental Surgery, Medical Faculty, RWTH Aachen University and performed according to the Directive 2010/63/EU of the European Parliament. Human tumour-free lung tissue was obtained from patients undergoing lobectomy due to cancer. The study was performed according to the Declaration of Helsinki and approved by the local ethics committee (EK 61/09) [27].

2.3. Cell isolation and culture (cell lines, primary cell isolation)

The human adenocarcinoma-derived epithelial lung cell line NCI-H441 (ATCC [HTB-174™]) was cultured in RPMI medium (PAN-Biotech GmbH, Aidenbach, DE) with 10 % FCS (PAN-Biotech GmbH) and 1 % Penicillin/Streptomycin (Sigma-Aldrich). Human primary epithelial lung cells were isolated using the Multi tissue dissociation kit 1 from Miltenyi Biotec (Bergisch Gladbach, DE). Small pieces (2–4 mm) of tissue were transferred into a C-tube (Miltenyi Biotec) containing the dissociation enzyme mix. Afterwards, the tissue was dissociated using the gentleMACS™ Octo Dissociator (Miltenyi Biotec). Samples were further processed by several centrifugation steps and the use of MACS SmartStrainers from Miltenyi according to the manufacturer. Subsequently, fibroblasts were depleted using CD90 Microbeads (130-096-253, Miltenyi Biotec) and epithelial cells were purified using CD326 (EpCAM) MicroBeads (130-061-101, Miltenyi Biotec) following the manufacturer's protocol. Selected cells were cultured in cell culture flasks (Greiner bio-one, Kremsmünster, AUT) coated with a coating solution containing 0.01 mg/ml Fibronectin (PromoCell, Heidelberg, DE) and 0.03 mg/ml collagen type 1 (Sigma-Aldrich) in PBS (Sigma-Aldrich). Small Airway Epithelial Cell Growth Medium from PromoCell was used as growth medium. Validation of cell type purity was done by flow cytometric analysis (see according chapter).

2.4. Substrate transfection and shedding assay

Activity assays with overexpressed substrates coupled to alkaline phosphatase (AP) were used to measure the relative shedding activation of the metalloproteinases ADAM10 and ADAM17. AP-coupled betacellulin (BTC) served as a substrate for ADAM10 and AP-coupled transforming growth factor α (TGFα) for ADAM17. In essence, 1×10^5 H441 cells were seeded in 24-wells. Transient transfection with a pcDNA 3.1 plasmid, encoding for TGFα-AP or BTC-AP was performed with Lipofectamine 3000 (Thermo, Waltham, USA) according to the manufacturer's protocol (Lipofectamine™ Reagent protocol). After 24 h, cells were washed, and fresh complete cell culture medium was added. After another 24 h, cells were treated with activators or inhibitors, or stretched as indicated. The shedding activity was determined by measuring the AP activity in the cell lysates and supernatant (lysis buffer: 50 mM Tris; 137 mM NaCl; 2 mM EDTA; 10 mM 1,10-phenanthroline; 1 % Triton X-100; pH 7.5). The AP activity was continuously measured at 405 nm with a microplate reader SpectraMax iD3 (Molecular Devices, San Jose, USA) by adding *p*-Nitrophenyl phosphate (PNPP) solution (Thermo). Then, the slope (change of absorption at 405 nm/s) was calculated. The amount of ADAM10 and ADAM17 activity was calculated as PNPP substrate turnover (AP activity) in the supernatant in relation to the total turnover in supernatant plus cell lysate.

2.5. Lentiviral transduction

Lentiviral transduction of short hairpin RNA (shRNA) was performed with the MISSION® shRNA system from Sigma-Aldrich as described

before [28]. For Piezo1 knockdown the pLKO.1-puro plasmid TRC number 0000141714 (sequence: GCTGCTCTGCTACTTCATCAT) was used. The pLKO.1-puro non-mammalian shRNA control plasmid DNA (SHC002) served as control. For production of recombinant lentiviruses, HEK293T cells in a 25 cm cell culture dish were cotransfected with 12.5 μg of the specific pLKO.1-puro plasmid, 8.13 μg of psPAX2 (plasmid 12260, Addgene, Watertown, USA) and 4.375 μg of pMD2.G (plasmid 12,259, Addgene) using 50 μl jetPEI® DNA transfection reagent (Polyplus-transfection, Illkirch France). Medium was changed after 24 h, and lentivirus containing supernatants were harvested after another 48 h. Ultracentrifugation at 50000 ×*g* for 2 h was used to concentrate lentiviral particles 500-times. Finally, the pellet was resuspended in PBS (Sigma-Aldrich). Lentivirus concentrate (5 μl) was added to 0.5×10^6 cells in 2 ml culture medium supplemented with polybrene (4 μg/ml, Sigma-Aldrich). Selection was done with puromycin dihydrochloride (Sigma Aldrich).

2.6. Piezo1- Western blotting

Knockdown and control cells were harvested and counted. 1×10^6 cells were lysed with 250 μl RIPA buffer (10 mM Tris buffer (pH 8.0), 140 mM NaCl, 1 mM EDTA, 0.1 % sodium deoxycholate, 0.1 % SDS, 1 % Triton X-100, 1 mM PMSF, 8 mM β-mercaptoethanol and cOmplete proteinase inhibitor cocktail) for 1 h at 4 °C. Samples were centrifuged at 16,000 x*g* for 20 min at 4 °C. 15 μl lysate was mixed with 5 μl reducing loading buffer (200 mM Tris-HCl (pH 6.8), 8 % (w/v) SDS, 40 % glycerol, 16 % (v/v) β-mercaptoethanol, 400 mM DTT and 0.01 % (*w/v*) bromophenol blue). Samples were separated by SDS-PAGE in a 4–15 % Mini-PROEAN TGX stain-free gel (Bio-Rad, Hercules, USA), and transferred to polyvinylidene difluoride (PVDF) membranes (Millipore, Immobilon-FL, Sigma). Membranes were blocked using 5 % (w/v) non-fat dry milk in TBST (50 mM Tris, 150 mM NaCl, 0.1 % Tween, pH 7.4) for 20 min at room temperature. Primary antibodies (mouse anti-Piezo1 (1:1000), Thermo, MA5-32876, clone 2–10; mouse anti-Transferrin receptor 1 (1:1000), Thermo, 13-6800, clone H68.4) diluted in TBST with 1 % (w/v) bovine serum albumin (BSA, AppliChem GmbH, Darmstadt, DE) were incubated overnight at 4 °C. Membranes were washed three times with TBST, followed by incubation with the secondary antibody (DyLight-680-conjugated anti-mouse (1:20000)), Thermo (35519); horse radish peroxidase (HRP)-conjugated anti-mouse (1:200000) from Jackson ImmunoResearch Laboratories, Inc. (115-036-003, Pennsylvania, USA) for 1 h at room temperature. After washing once with TBST and two times with TBS proteins were detected using Odyssey 9120 imager system (LI-COR) and the ChemiDoc MP Imaging System (Bio-Rad). The band intensities were measured with the software Image studio Lite Version 5.2 (LI-COR, Lincoln, U.S.A.).

2.7. Quantitative PCR (qPCR)

The mRNA expression levels were measured by quantitative PCR and normalised to the mRNA expression levels of the chosen reference genes. TATA-binding protein (TBP) and DNA topoisomerase I (TOP1) were identified as suitable reference genes using CFX Maestro Software 1.1 (Bio-Rad). RNA was extracted with the RNeasy Kit (Qiagen, Hilden, Germany) and was quantified photometrically (NanoDrop, Peqlab, Erlangen, Germany). RNA was reverse transcribed using PrimeScript™ RT Reagent Kit (Takara Bio Europe, St-Germain-en-Laye, France) according to manufacturers' protocols. PCR reactions were then performed in duplicates of 10 μl volume containing 1 μl of cDNA template, 5 μl iTaq Universal SYBR Green Supermix (Bio-Rad), 3 μl H_2O and 0.5 μl forward and reverse primer. A list of all used primers and corresponding annealing temperatures is presented in Supplementary Table 1. All PCR reactions were run on the CFX Connect Real-Time PCR Detection System (Bio-Rad) using following protocol: 40 cycles of 10 s denaturation at 95 °C, followed by 10 s annealing at the listed temperatures and 15 s amplification at 72 °C. We utilised the LinRegPCR version 2020.0 software to determine the efficiency from the uncorrected RFU values [29]. Relative quantification was performed with the CFX Maestro Software 1.1 (Bio-Rad).

2.8. ELISA

Supernatants of stimulated cells were harvested and cleared from cell debris by centrifugation (5 min, 4 °C; 16,000 g). Released soluble JAM-A (JAM-A ELISA kit, SinoBiological, Beijing, China) or amphiregulin (Human Amphiregulin DuoSet ELISA, R&D Systems, Minneapolis, USA) were quantified per ELISA as recommended by the manufacturers. As substrate for the chromogenic reaction the BM Blue POD substrate (Roche, Basel, Switzerland) was used.

2.9. Immunocytochemistry and immunofluorescence microscopy analysis

Cells grown on glass coverslips were fixed with ice-cold methanol for 3 min. Afterwards they were dried and directly used for staining or stored at 4 °C for no longer than 7 days. Samples were blocked for 30 min at room temperature with 5 % (w/v) BSA (SERVA, Heidelberg, Germany) in PBS. Primary and secondary antibodies were diluted in 1 % BSA (w/v) in PBS and incubated with the sample at room temperature for 1 h each with a washing step in PBS between primary and secondary antibody. Samples were mounted on glass slides with Mowiol (Carl Roth, Karlsruhe, Germany). Rat monoclonal DECMA-1 antibody against E-cadherin from Sigma Aldrich (U3254) was used in dilution of 1:200 and mouse monoclonal antibody against JAM-A from Hycult Biotech (HM2099-100UG) in dilution of 1:100. Alexa Fluor 488-conjugated secondary mouse (A-11029) and 555-conjugated secondary rat (A-21434) antibodies were from Invitrogen and diluted in concentrations of 1:1000 and 1:500, respectively. Nuclei were stained with Hoechst 33342 from Thermo Fisher Scientific. Microscopy analysis was performed with an Axio Imager M2, equipped with an Apotome.2 and using an AxioCam 305 camera, filter sets 38,43 and 49, a HXP 120C as light source and a Plan-Apochromat 20×/0.8 DIC objective (Carl Zeiss, Jena, DE). Images were processed using Zen 3.3 blue edition (Carl Zeiss) and ImageJ open source software (National Institutes of Health, Bethesda, MD, USA). For relative quantification of the apparent adhesion width, 5 fields of view were selected and the width of 20 cell-cell adhesions was measured per field of view. Finally, the adhesion width was given as the mean value from the 100 measured cell-cell adhesions. The number of cells per field of view was quantified counting the cell nuclei.

2.10. Stretching chambers and mechanical stretching

Elastic stretching chambers were prepared of cross-linked polydimethylsiloxane (PDMS, Sylgard 184, weight ratio 10:1, 20:1, 40:1 or 50:1 base to cross-linker) as described before [30]. PDMS was carefully poured into chamber molds and cross-linked for 16 h at 60 °C. Produced chambers exhibited a Young's modulus of either 15, 50, 500 or 1200 kPa. Chambers were sterilised with 2-propanol (Carl Roth GmBH + Co. KG) and then coated for 0.5 h with Collagen G (Sigma Aldrich) in PBS in a ratio of 1:100. Then, 1.25×10^5 cells/cm^2 were seeded on each PDMS chamber in presence of 500 μl RPMI medium. A custom-made stretcher 6× device with a linear stepper motor (MT63, Steinmeyer Mechatronik GmbH, Dresden, Germany) was used as described before [31,32]. Chambers were fixed into the stretching device and pre-stretched to evade sagging of the chamber. The stretcher device, together with unstretched control samples were placed in the incubator at 37 °C. An associated program allowed us to individually set stretch amplitudes and times. Stretch amplitudes were increased stepwise by 10 % up to a maximum of 40 % every 15 or 60 min, depending on the experiment (Fig. 5b, c).

2.11. Isolated perfused murine lungs

Lungs were prepared from sacrificed mice as described [33]. For a baseline, lungs were ventilated for 15 min with a respiratory rate of 90 breaths per minute, an end-inspiratory pressure of −8 cm H_2O and an end-expiratory pressure of −3 cm H_2O, resulting in a tidal volume of ~250 μl. Afterwards, mice were either treated intratracheally with 50 μl containing SalB (300 μM) or DMSO as control and normal ventilation was continued for 30 min. Subsequently, mice received high-pressure ventilation with an end-inspiratory pressure of −22.5 cm H_2O and an end-expiratory pressure of −3 cm H_2O, resulting in a tidal volume of ~500 μl for 3 h. Perfusion of pulmonary vasculature was performed with perfusing buffer containing polysuccinated bovine gelatin and various supplements including sodium phosphate and sodium hydrogen carbonate as described before [34].

2.12. Flow cytometric analysis

Cells isolated from human lungs were stained against human Fibroblast (PE, 130–100-137), human CD326 (EpCAM) (APC, 130-111-117) and CD31 (VioBlue®, 130-117-227) from Miltenyi Biotec. Isotyp VioBLue (130-113-454), Isotyp PE (130-113-450) and Isotyp APC (130-113-446) from Miltenyi Biotec (Bergisch Gladbach, DE) were used as controls. The staining procedure was done according to the manufacturer's protocol. The fluorescence signal was measured by flow cytometry (LRS Fortessa, BD Biosciences, Heidelberg, DE) and analysed with FlowJo 10.2 software (Tree Star, Inc., Ashland, USA).

2.13. Statistics

Quantitative data are given as mean plus standard deviation (SD) calculated from a minimum of three independent experiments. Statistics were performed using the generalised mixed model analysis (PROC GLIMMIX, SAS 9.4, SAS Institute Inc., Cary, North Carolina, USA) and assumed to be from either normal, beta or lognormal distribution with the day of experiment conduction as random to assess differences in the size of treatment effects across the results. Residual plots and the Shapiro-Wilk test were used as diagnostics. If heteroscedasticity was given (according to the covtest statement) the degrees of freedom were attuned by the Kenward-Roger approximation. All p-values were adjusted for multiple comparisons by the false discovery rate (FDR). Normalised data of the experiments with primary human lung epithelial cells was analysed using a one sample *t*-test against the hypothetical value of 1 (GraphPad Prism 8, GraphPad Software, La Jolla, USA). EC_{50} values were calculated using GraphPad Prism 8 (GraphPad Software, La Jolla, USA), in which a dose-response curve was fitted. For immunofluorescence images, the mean values of each independent experiment were determined from 5 quantified images and then taken as basis for statistical analysis. All p-values $<.05$ were considered significant.

3. Results

3.1. The Piezo1 activator Yoda1 promotes ADAM10- and ADAM17-specific substrate cleavage in epithelial cells

Piezo1 has been shown to play an important role in sensation of different mechanical stimuli in a variety of cell types [6,35]. Previous studies demonstrated that ADAM10 can be activated by the small molecule activator of Piezo1, Yoda1, in endothelial cells [26]. We wondered whether this is also the case in epithelial cells and whether ADAM17, another important metalloproteinase, can also be activated by Yoda1. To measure the relative shedding activity of ADAM10 and ADAM17 we used activity assays with overexpressed substrates coupled to alkaline phosphatase (AP) (Fig. 1a). Human lung epithelial H441 cells were transiently transfected with the ADAM10 substrate BTC-AP and the ADAM17 substrate TGFα-AP. They were then stimulated with different concentrations of Yoda1. ADAM10 shedding activity was significantly increased at a concentration of 3 μM Yoda1 with a half maximal effective concentration (EC_{50}) of 14.5 μM. Of note, ADAM17 was substantially more sensitive to Yoda1 than ADAM10 with an EC_{50} of 1.5 μM Yoda1 (Fig. 1b, c).

Next, we examined different time points of ADAM activation to determine adequate conditions for further experiments. We could detect a significant increase in shedding activity of ADAM10 and ADAM17 already after 30 min of Yoda1 stimulation (Fig. 1d, e). To illustrate the relative changes in shedding activity, we additionally plotted the data normalised to the corresponding control (Suppl. Fig. 1). Induction of ADAM10 activity was strongest at 1 h and 1.5 h with a, 6-/ or 5-fold increase, and decreased after 2 h. In contrast, relative increase of shedding activity of ADAM17 stayed constant.

For further experiments, we chose to stimulate H441 cells with 10 μM Yoda1 for 1.5 h. To additionally validate the ADAM specificity of the Yoda1-induced effect, we preincubated cells with GI or TAPI1, which are inhibitors for ADAM10 and ADAM17, respectively [36]. Then, H441 cells were treated with Yoda1, DMSO (negative control), PMA or ionomycin. PMA and ionomycin served as positive controls for selective activation of either ADAM17 or ADAM10, respectively (the selectivity of both controls was again demonstrated in Suppl. Fig. 2). In contrast to PMA and ionomycin, Yoda1-induced activation of both ADAM10 and ADAM17. Yoda1-induced shedding of ADAM10 and ADAM17 substrates was significantly suppressed by the corresponding inhibitors, giving further evidence of the ADAM specificity (Fig. 1f, g).

Since Yoda1 and PMA both promote ADAM17 activation we next asked for possible differences in the activation pathway. Since protein kinase C isoforms are well known to be activated by PMA and by intracellular free calcium, we next applied the pan-specific protein kinase C inhibitor BIM2. As described earlier, BIM2 can suppress PMA-induced ADAM17 activation (Suppl. Fig. 3). By contrast, Yoda1 induced ADAM17 activation is not affected by the inhibition of PKCs. Thus, partially overlapping but also distinct signalling events contribute to ADAM17 activation in response to PMA on the one hand and Yoda1 on the other.

Together, these findings suggest that activation of Piezo1 via the small molecule Yoda1 increases the shedding activity of ADAM10 not only in endothelial, as previously reported [26], but also in epithelial cells. Additionally, our data demonstrate for the first time that also the shedding activity of ADAM17 can be induced by Yoda1.

3.2. Yoda1 promotes ADAM10 and ADAM17 activity via Piezo1

To further investigate the role of Piezo1, we generated Piezo1 knockdown cells by transducing H441 cells with a lentivirus coding for shRNA against Piezo1 or untargeted control shRNA. The knockdown was confirmed at the protein level by western blot and at the mRNA level by qPCR (Fig. 2a–c, Suppl. Fig. 4). Cells were treated for 1.5 h with Yoda1, DMSO (negative control) or PMA/ionomycin (positive controls). ADAM activity was then measured using the activity assays described above. We found that, the Yoda1-induced ADAM10 and ADAM17 activation was significantly reduced by the Piezo1 knockdown. In contrast, the increased ADAM10 and ADAM17 activities induced by ionomycin or PMA, respectively, was not influenced by the Piezo1 knockdown (Fig. 2d, e). Together, these results prove that the Yoda1-induced activation of ADAM10 and ADAM17 is dependent on Piezo1.

3.3. Activation of Piezo1 induces shedding of amphiregulin in epithelial cells

Amphiregulin (AREG) is a prominent substrate of ADAM17. Given the importance of the ADAM17-AREG axis in epithelial proliferation, resistance against apoptosis and tumour growth, we wondered whether AREG expression and release in pulmonary epithelial cells could be influenced by the activation of Piezo1 [37,38]. We stimulated H441 cells

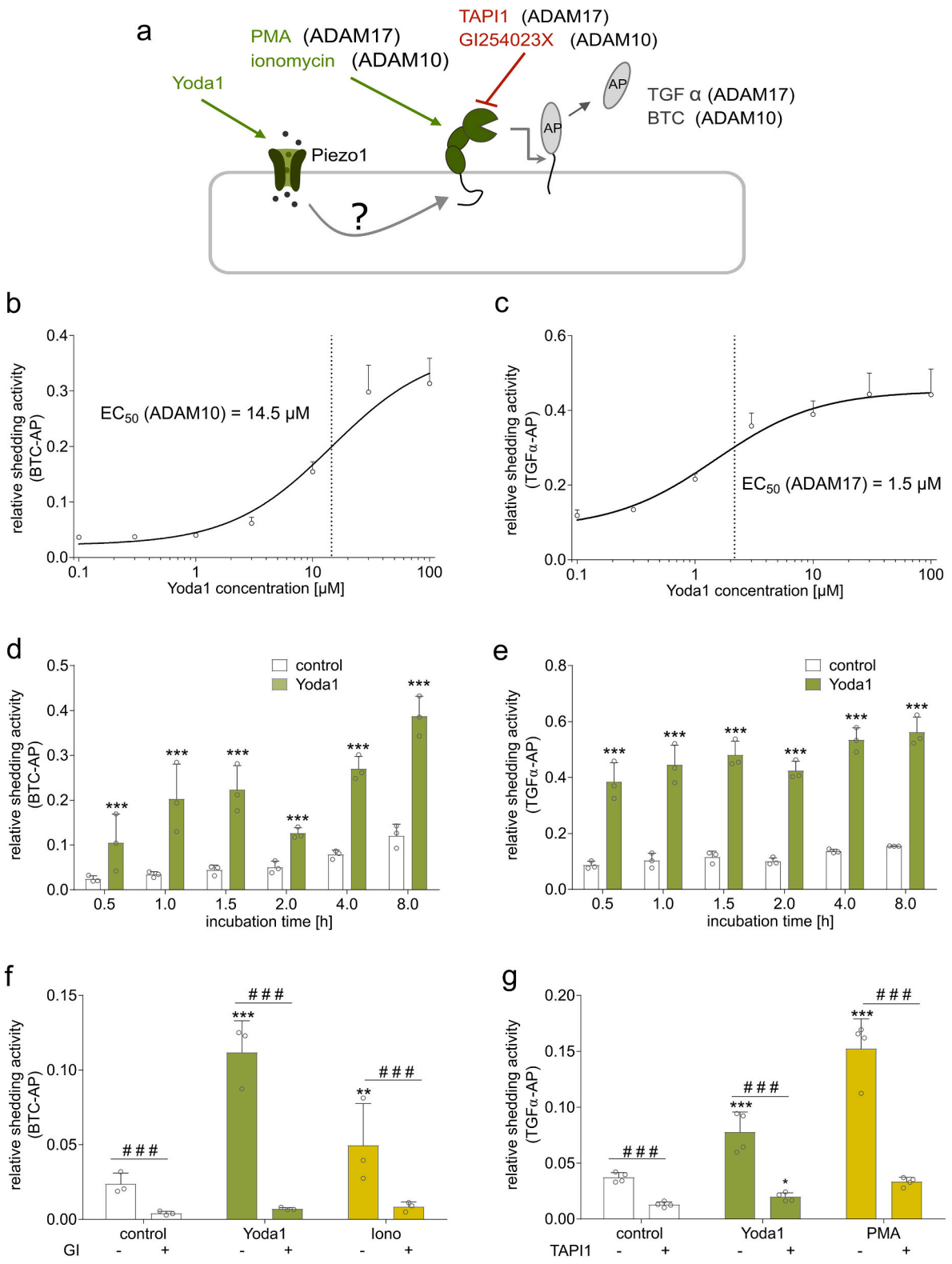

Fig. 1. Yoda1 induces ADAM10- and ADAM17-specific substrate cleavage in the lung epithelial cell line H441. Experimental setup to test the hypothesis whether Yoda1 stimulates ADAM10 and ADAM17 shedding (a). H441 cells were transfected to express specific substrates for ADAM10 and ADAM17 coupled to alkaline phosphatase (AP). BTC was used as a substrate for ADAM10 and TGFα for ADAM17. Ionomycin and PMA were used as established and specific activators for ADAM10 and ADAM17, respectively. To specifically inhibit ADAMs, cells were pretreated with GI or TAPI (a). Subsequently, cells were stimulated with the indicated concentrations of Yoda1 for 1.5 h (b, c) or a fixed concentration of 10 µM for different time periods (d, e) before the shedding activity of ADAM10 (b, d) and ADAM17 (c, e) was determined. ADAM specificity was tested by pretreating cells with ADAM specific inhibitors GI (10 µM) (f) and TAPI1 (40 µM) (g) for 30 min and subsequently stimulating cells for 1.5 h with Yoda1 (10 µM) or with ionomycin (1 µM) for ADAM10 activation or PMA (100 nM) for ADAM17 activation. Afterward, ADAM10 and ADAM17 substrate cleavage was measured. Quantitative data are shown as mean + SD of at least three independent experiments. Statistical differences to the control are indicated by asterisks (* $p < .05$, ** $p < .01$, *** $p < .001$) and differences between the treatments are indicated by hashes (# $p < .05$, ## $p < .01$, ### $p < .001$).

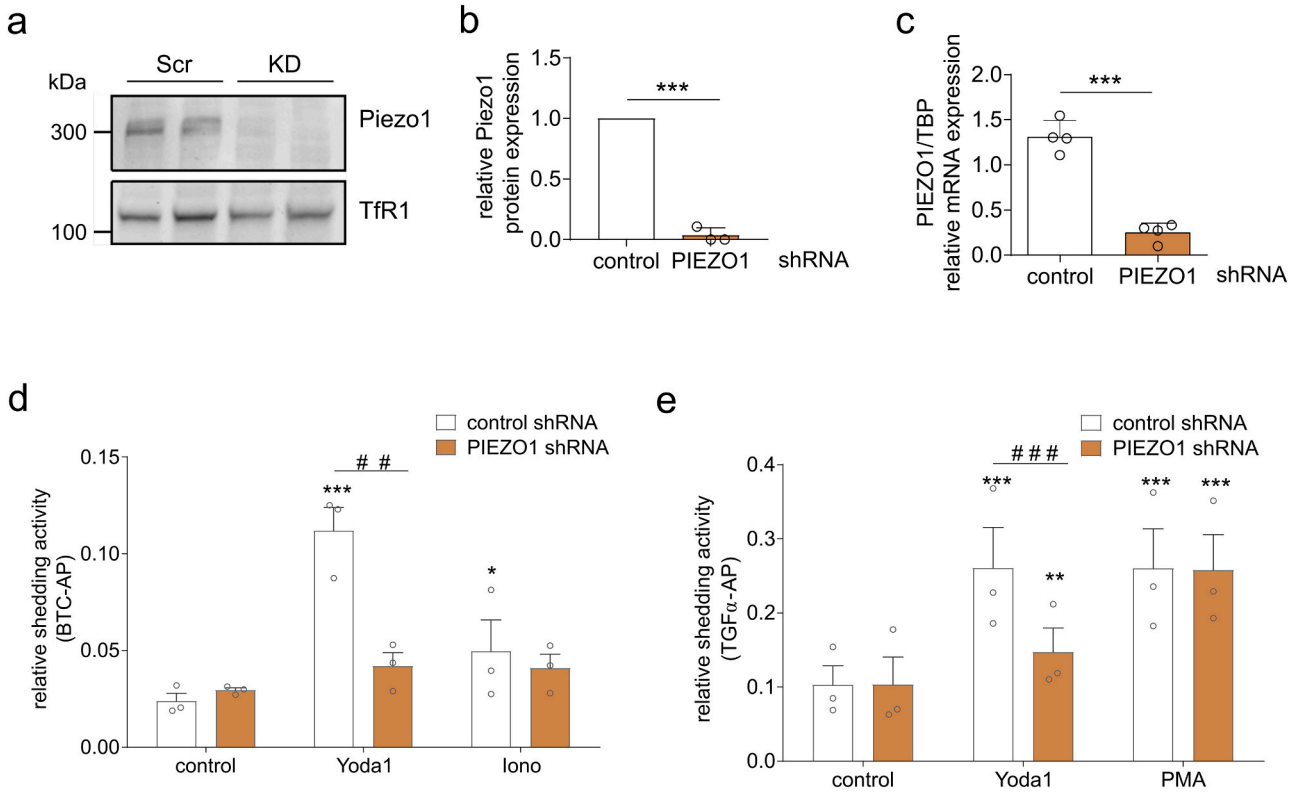

Fig. 2. Yoda1-induced activation of ADAM proteinases is dependent on Piezo1. The involvement of Piezo1 was studied by a shRNA-mediated knockdown of Piezo1. Untargeted shRNA served as control. The knockdown was validated via western blot (a, b, for uncropped western blot see Suppl. Fig. 4) and qPCR (c). Piezo1 protein expression is shown relative to the loading control TfR1 and was normalised to the respective shRNA control (b). H441 cells with or without Piezo1 knockdown were stimulated with Yoda1 (10 μM) or PMA (100 nM) or ionomycin (1 μM) for 4 h. Subsequently, the shedding activity of ADAM10 (d) and ADAM17 (e) was tested via activity assays with overexpressed substrates coupled to alkaline phosphatase (AP). Quantitative data are shown as mean + SD of at least three independent experiments. Statistical differences to the control are indicated by asterisks (* $p < .05$, ** $p < .01$, *** $p < .001$) and differences between the treatments are indicated by hashes (# $p < .05$, ## $p < .01$, ### $p < .001$).

with Yoda1 and measured mRNA expression and release of soluble AREG via qPCR and ELISA, respectively. As expected, chemical activation of Piezo1 in epithelial lung cells led to an enhanced AREG release (Fig. 3a). This is in line with our finding that ADAM17 shedding activity is increased after Piezo1 activation. Intriguingly, the enhanced AREG release increased rapidly after 4 h stimulation. The mRNA expression of AREG was upregulated after 1 h of Yoda1 stimulation and increased gradually over time (Fig. 3b). Thus, activation of Piezo1 not only stimulates AREG shedding but also upregulates AREG gene expression at the transcriptional level leading to further increase of total AREG release. In contrast, only minor changes in gene expression of ADAM10 and ADAM17 were observed after Yoda1 stimulation (Suppl. Fig. 5).

To determine the role of ADAM17 in this process, we stimulated H441 cells with Yoda1 and PMA. In both instances, AREG release was significantly enhanced and could be suppressed by inhibition of ADAM17 with TAPI1, validating the critical involvement of ADAM17 (Fig. 3c). In Piezo1 knockdown cells, AREG release was strongly suppressed in comparison to control cells (Fig. 3d). Thus, chemical activation of Piezo1 in epithelial lung cells enhances expression and subsequent release of AREG. Again, this is associated with a Piezo1-dependent increase of ADAM17 activity.

In a subsequent experiment we asked whether a pulse of Yoda1 stimulation would be sufficient to induce activation of AREG shedding. We exposed cells to Yoda1 for 5 min, replaced the medium and then continued incubation without Yoda1 for 4 h. 5 min of Yoda1 exposure clearly increased AREG release even after removal of Yoda1 (Suppl. Fig. 6). The data suggest that continuous stimulation of Piezo1 is not necessary to maintain ADAM17-mediated AREG release for up to 4 h.

3.4. Piezo1 reduces epithelial cell junctions by inducing JAM-A shedding

Stability of cell junctions in epithelial monolayers has been shown to be crucial for the maintenance of epithelial cohesion and barrier function, and to balance cell proliferation processes. Prominent examples of epithelial cell junction proteins are E-cadherin, which is found in adherens junctions, and JAM-A, which is a component of tight junctions [39]. Both cell adhesion molecules are well known substrates of ADAM proteinases. While E-cadherin cleavage is mediated by ADAM10, JAM-A is predominantly shed by ADAM17 and to a lesser extent by ADAM10 [22,40]. Given that E-cadherin as well as JAM-A are substrates of ADAM proteinases, we wanted to test whether Yoda1-induced ADAM activation might influence cell junctions. Therefore, H441 cells were stimulated with Yoda1 for 2, 4 or 8 h and thereafter stained for E-cadherin and JAM-A. For both E-cadherin and JAM-A, the integrated fluorescence density was reduced after 4 h Yoda1 treatment in comparison to the control conditions, however this reduction was only significant for JAM-A (Fig. 4a–c). This effect on JAM-A became even more pronounced with a longer incubation period of 8 h (Suppl. Fig. 7). Considering the different sensitivity of both substrates JAM-A and E-cadherin for ADAM17 and ADAM10, respectively, this finding may indicate that ADAM17 activity is upregulated more prominently than ADAM10 activity. In contrast to AREG, gene expression of JAM-A and E-cadherin, were not increased after Yoda1 stimulation over time (Suppl. Fig. 8). To rule out effects on proliferation or cell death during this period of time cell counting and cell density measurements were performed and did not indicate any changes (Fig. 4d, Suppl. Fig. 9). Additionally, cell morphology seemed to be altered and stained cell-cell adhesions were reduced to a thinner line after Yoda1 treatment (Fig. 4e). This indicates

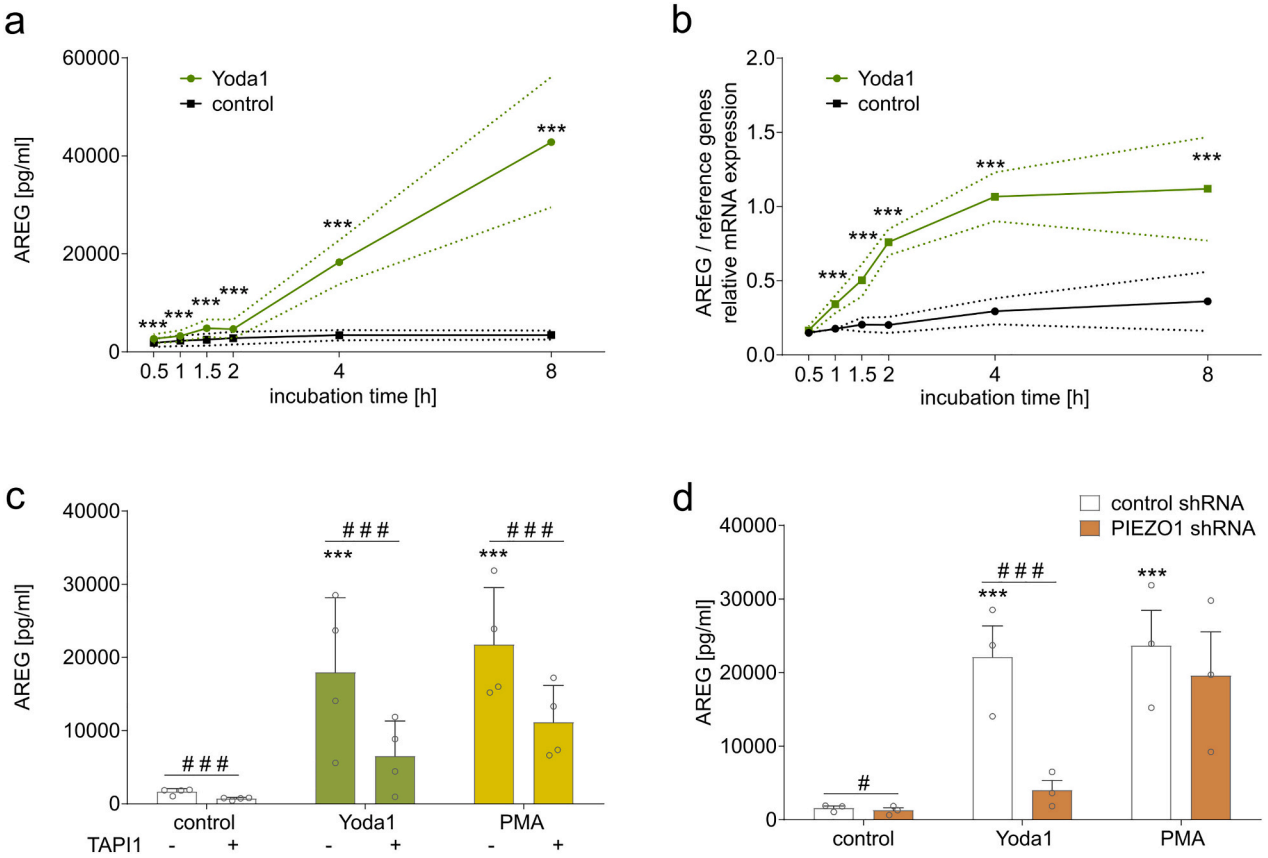

Fig. 3. Piezo1-dependent activation of amphiregulin shedding as a substrate of ADAM17 in H441 epithelial cells. H441 cells were stimulated with Yoda1 or corresponding control for 0.5 h, 1 h, 1.5 h, 2 h, 4 h or 8 h. Amphiregulin (AREG) release into the supernatant was measured by ELISA (a) and relative gene expression was analysed by qPCR (b). H441 cells were treated with or without the ADAM17 inhibitor TAPI1 (40 μM), subsequently stimulated with Yoda1 (10 μM) or PMA (100 nM) or left unstimulated for 4 h and finally investigated for AREG release (c). Piezo1 knockdown and control cells were treated with Yoda1 (10 μM) or PMA (100 nM) for 4 h after which the AREG release was measured (d). Quantitative data are shown as mean + SD of at least three independent experiments. Statistical differences to the control are indicated by asterisks (* $p < .05$, ** $p < .01$, *** $p < .001$) and differences between the treatments are indicated by hashes (# $p < .05$, ## $p < .01$, ### $p < .001$).

that Piezo1 stimulation might lead to a reduction of cell junction area induced by the increased shedding of JAM-A and possibly also E-cadherin by ADAM proteinases.

To verify these results, we further measured the amount of shed JAM-A by ELISA. In line with the immunofluorescence staining, JAM-A shedding was significantly increased with Yoda1. As expected, these effects could be abolished by TAPI1, and to some degree by GI (Fig. 4f). Overall, activation of Piezo1 induces downregulation of JAM-A and potentially also E-cadherin at epithelial cell junctions by proteolytic shedding via ADAM proteinases.

3.5. *Mechanical stretching promotes ADAM17 activity via Piezo1*

Alveolar epithelial cells are subjected to stretching due to alveolar inflation. Previous research has shown that epithelial stretch can trigger Ca^{2+} influx through Piezo1 [14,41]. Therefore, we utilised a stretching device that allowed us to cultivate H441 cells on flexible chambers made of cross-linked PDMS and to stretch them with defined amplitudes [32] (Fig. 5a). Stretching with increasing amplitudes for 1.5 h led to a significantly enhanced shedding activity of ADAM17 in H441 control cells as determined by the cleavage of the overexpressed ADAM17 substrate. This response was significantly reduced in Piezo1 knockdown cells (Fig. 5b). We also determined the AREG release by ELISA. The amount of released AREG was significantly increased after stretch (Fig. 5c). Interestingly, AREG release was only slightly promoted when cells on the PDMS membrane were stimulated with Yoda1 instead of stretching. This is in contrast to the results obtained in Yoda1-simulated cells that were grown on normal plastic dishes. qPCR measurements revealed that relative gene expression of AREG in cells on PDMS membranes could not be increased by stretch or by Yoda1 (Fig. 5d). Without upregulation of AREG expression Yoda1 stimulation can induce only a smaller increase of AREG release. Gene expression of Piezo1 and ADAM17 was not changed by stretch (Suppl. Fig. 10). A possible explanation for the mitigated mRNA induction and release of AREG in H441 cells grown on PDMS is the change in substrate stiffness or surface chemistry. In accordance, H441 cells grown on PDMS with varying stiffness showed a drastically suppressed AREG release and mRNA induction by Yoda 1 in comparison to cells grown on cell culture plastic (Fig. 5e, f) whereas mRNA expression of Piezo1 and ADAM17 as well as Piezo1 protein expression were only slightly affected, if at all (Suppl. Figs. 11, 12).

3.6. *Induction and release of AREG in H441 and primary human lung cells can be suppressed by Piezo1 inhibition*

Recently, salvianolic acid B (SalB) was described as Piezo1 inhibitor [17]. To study SalB in our experimental setup H441 cells were pretreated with different concentrations of the inhibitor and then stimulated with the Piezo1 agonist Yoda1. Piezo1-mediated increase of AREG shedding and gene expression was significantly suppressed with a SalB concentration of 30 μM (Fig. 6a,b). More profound reduction of AREG release and gene induction was seen with a high concentration of 300 μM SalB. Gene expression of ADAM17 and Piezo1 was not influenced by SalB (Fig. 6c, d). Furthermore, PMA-induced AREG release was not

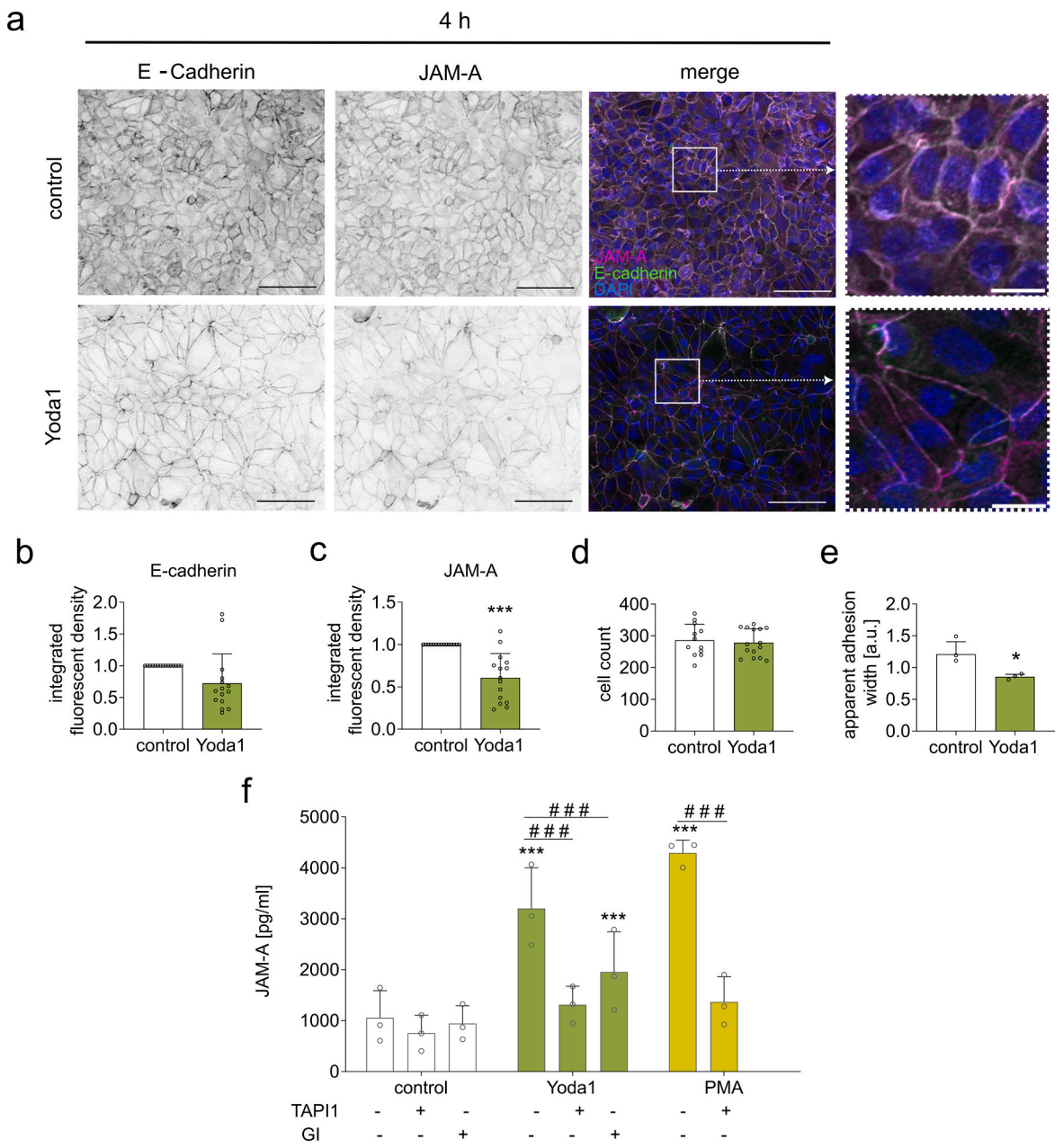

Fig. 4. Piezo1 activation leads to the shedding of cell-cell junction molecules, E-cadherin and JAM-A. H441 cells were stimulated with Yoda1 (10 μM) or DMSO as control for 4 h and subsequently stained for JAM-A and E-cadherin. Data are shown as representative single immunofluorescence images in inverted scale and double fluorescence images with nuclear staining via DAPI (a) and quantification of fluorescence (b, c). The number of cells per field of view was quantified counting the cell nuclei (d). Five fields of view for each of three independent experiments were analysed. Apparent adhesion width was measured for 100 cell-cell adhesions for each independent experiment (e). JAM-A release of H441 cells treated with or without TAPI1 (40 μM) or GI (10 μM), and subsequently stimulated for 4 h with Yoda1 (10 μM) or PMA (100 nM), was measured by ELISA (f). Quantitative data are shown as mean + SD of at least three independent experiments. Statistical differences to the control are indicated by asterisks (* $p < .05$, ** $p < .01$, *** $p < .001$) and differences between the treatments are indicated by hashes (# $p < .05$, ## $p < .01$, ### $p < .001$). Scale bars represent 80 μM and 20 μM in zoom pictures.

supressed by SalB indicating that the inhibition of the Yoda1-induced response was in fact due to Piezo1 inhibition and not to an off-target effect (Suppl. Fig. 13). To investigate whether these processes would also occur in a more physiological setting, we isolated primary epithelial cells from human lungs. After cell type separation, the purity was validated by flow cytometry, showing that over 90 % of cells were positive for the epithelial cell marker CD326 (Suppl. Fig. 14). Also, in primary epithelial cells there was an increased AREG release upon stimulation with PMA or upon Piezo1 stimulation with Yoda1. As expected, both responses could again be suppressed by the ADAM17 inhibitor TAPI1. By contrast, the Piezo1 inhibitor SalB only reduced AREG release induced by Yoda1 but not that induced by PMA (Fig. 6e). These data again confirm that SalB suppresses Piezo1-mediated responses but has no unspecific effects on AREG release. For comparison, we analysed the transcriptional regulation of AREG revealing a slight increase by Yoda1 and even a reduction by PMA treatment (Fig. 6f). Overall, these findings indicate that AREG is constitutively expressed in human primary lung epithelial cells and that its release can be enhanced by Piezo1-mediated ADAM17 activation.

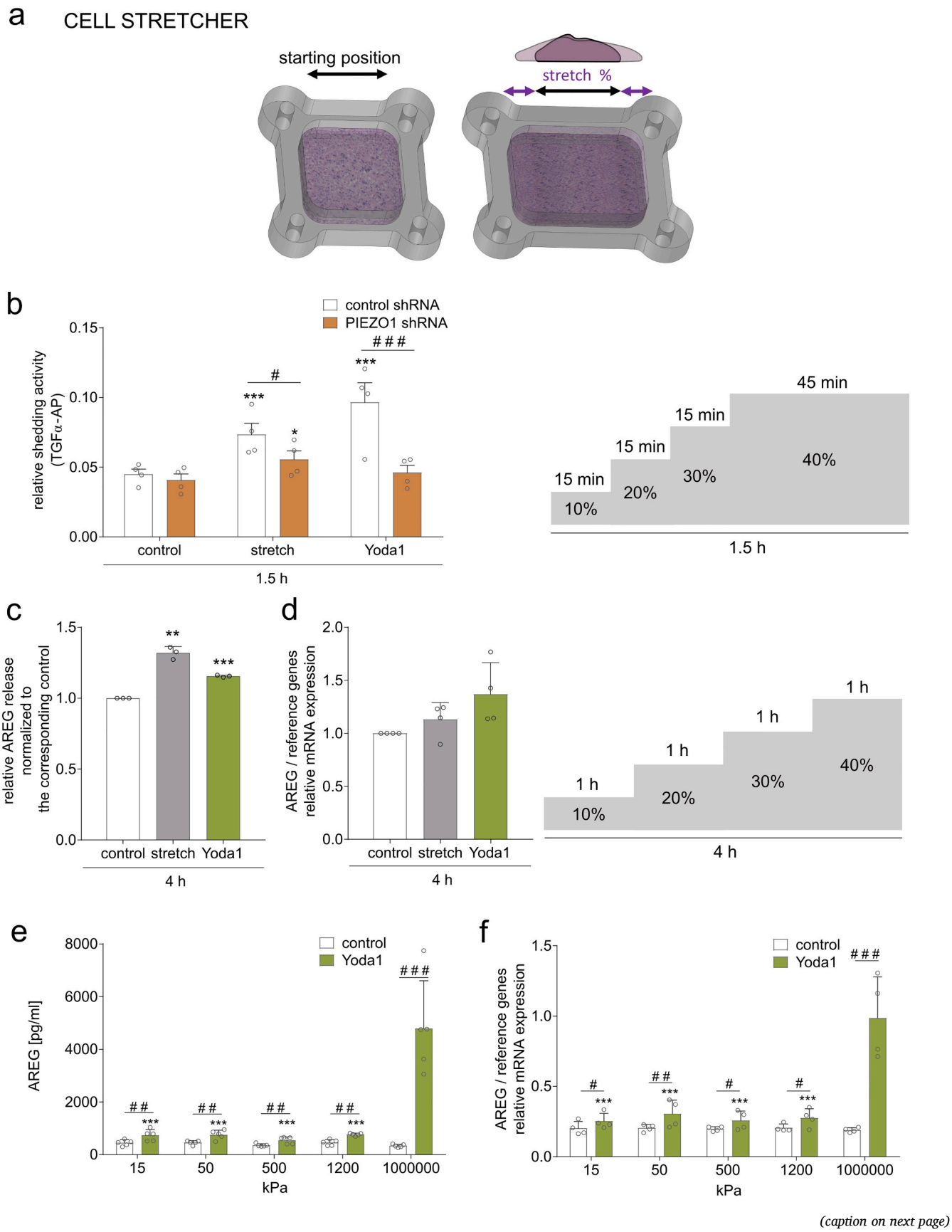

(caption on next page)

Fig. 5. ADAM17 activation via Piezo1 can be induced by mechanical stretch in dependence to stiffness. H441 cells were cultivated for 2 days on PDMS chambers (50 kPa) allowing uniaxial stretching with defined amplitudes (a). H441 cells transduced to express control shRNA or Piezo1 shRNA, were stretched for 1.5 h according to a stretch protocol (right) with increasing stretch amplitudes or stimulated with Yoda1 (10 μM) or DMSO without stretching. The relative ADAM17 shedding activity was measured by an activity assay with an overexpressed substrate (TGFα) coupled to alkaline phosphatase (AP) (b). The release and expression of endogenous AREG from H441 cells, either stretched for 4 h according to a stretch protocol (right) or stimulated with Yoda1 (10 μM) or DMSO without stretching, was measured by ELISA (c) or qPCR (d). H441 cells were cultivated on PDMS gels exhibiting an elasticity of 15, 50, 500 or 1200 kPa or on plastic (1 GPa, control). Then, H441 cells were stimulated with Yoda1 (10 μM) or DMSO. Subsequently, AREG release was measured by ELISA (e) and AREG mRNA expression via qPCR (f). Quantitative data are shown as mean + SD of at least three independent experiments. Statistical differences to the control are indicated by asterisks (* $p < .05$, ** $p < .01$, *** $p < .001$) and differences between the treatments are indicated by hashes (# $p < .05$, ## $p < .01$, ### $p < .001$).

3.7. High pressure ventilation promotes alveolar AREG release ex vivo

Mechanical activation of Piezo1 in the lung may play a role in high pressure ventilation, which can promote the development of acute respiratory distress syndrome (ARDS) [42]. Therefore, we performed experiments in the isolated perfused lung (IPL) applying high pressure ventilation to murine lungs (Fig. 7a). Previous studies had shown increased gene expression of AREG after high pressure ventilation in an IPL system [43]. We therefore wanted to test, whether this effect might be initially induced by Piezo1 activation and would also influence the alveolar release of AREG. Normal non-ventilated lungs were compared to high pressure ventilated lungs that had been intratracheally pretreated with or without the Piezo1 inhibitor SalB. On the gene expression level we could confirm the induced mRNA expression of AREG upon high pressure ventilation (Suppl. Fig. 15). However, this was not significantly affected by the pretreatment with SalB. It is likely that many different cell types in the lung tissue apart from epithelial cells can upregulate AREG mRNA expression. It is therefore questionable whether an effect of SalB can be expected since the inhibitor was applied via the airways to the epithelial layer only. To study the release of AREG from the alveolar lining cells more locally, bronchoalveolar lavage fluid (BALF) was prepared and investigated for AREG levels. Compared to non-ventilated lungs, high pressure ventilated lungs contained significantly more released AREG. This response was suppressed by administration of SalB (Fig. 7b). The alveolar release of JAM-A was also increased after high pressure ventilation. This response was less pronounced, but still significant and could be partially suppressed by Piezo1 inhibition (Fig. 7c). Thus, the release of the ADAM17 and ADAM10 substrates, AREG and JAM-A, into the alveolar space of the lung is enhanced by mechanical stimulation of epithelial cells via Piezo1.

4. Discussion

Piezo1 is a critical mechanoreceptor which is present in lung epithelial cells. Our study demonstrates that mechanical activation of Piezo1 drives the activation of the metalloproteinases ADAM10 and ADAM17 that are known to shed surface molecules relevant for inflammation, permeability control and cell proliferation. Of the ADAM17 substrates, we investigated the consequences of Piezo1 activation on the epithelial growth factor AREG in more detail. We could show that Piezo1 activation induced both AREG gene expression and AREG shedding from the cell surface. In parallel, we found that the constitutively expressed junctional molecule JAM-A is shed in response to Piezo1 activation in an ADAM10/17-dependent manner. This is associated with a reduced presence of JAM-A in cell junctions. Finally, we provide first evidence that the Piezo1-ADAM10/17 pathway is induced during high pressure ventilation of murine lungs.

Activation of Piezo1 promotes the activity of both metalloproteinases, ADAM10 and ADAM17. This was evidenced by the use of selective substrates (TGFα and BTC) and by the use of proteinase inhibitors allowing to discriminate the activities of both ADAMs. Of note, ADAM17 is more potently upregulated by activation of Piezo1 via Yoda1 than ADAM10. Piezo1-mediated ADAM10 activation on endothelial cells has been described by a previous study in which mechanical shear stress was used as a stimulus [26]. We here demonstrate that also ADAM17 is mechanically activated in stretched epithelial cells via Piezo1. As shown before, ADAM10 and ADAM17 can be specifically activated on a posttranslational level by the chemical agents ionomycin, a Ca^{2+} ionophore, and PMA, a PKC activator, respectively [24,25]. Although this indicates that the activation pathway for either proteinase differs, chemical and mechanical activation by Piezo1 and hence Piezo1-dependent Ca^{2+} influx seems to upregulate the activity of both proteinases. For now, we can only speculate about the exact process how Piezo1 stimulation leads to ADAM activation. It is known that increase of intracellular calcium can induce phospholipid translocation in the plasma membrane by calcium-dependent phospholipid scramblases. This results in an exposure of phosphatidylserine on the outer membrane leaflet [44]. This process has been associated not only with increased apoptosis but also with a transiently increased activation of ADAM17 [45,46]. It has been proposed that this activity regulation is brought about by a conformational change of the proteinase on the cell surface [47]. It is not yet clear whether ADAM10 is as sensitive to the phosphatidylserine exposure [44], but a reduced sensitivity might explain why ADAM10 is less potently upregulated by Yoda1. However, several other mechanisms could also be involved. This includes regulation of the proteinases via adaptor proteins. ADAM17 interacts with iRhom1 or 2 that are not only relevant for transport and maturation of the proteinase but also for activity regulation at the cell surface by intracellular phosphorylation [48]. We could already show in a previous work that expression of iRhom1 can be mechanically induced by shear stress in primary endothelial cells [49]. Moreover, Piezo1 activation can lead to ATP release via pannexin-1 in lung epithelial cells. The released ATP could activate purinergic P2X or P2Y receptors in an auto- or paracrine fashion [14]. Interestingly, activation of ADAMs through P2X7 was already shown in keratinocytes where it led to an increased migration [50]. Finally, it has been shown that Yoda1 can activate the extracellular signal regulated kinase (ERK1/2) signalling [51], that in turn can stimulate ADAM17 activity [52]. Soluble AREG shed by ADAM17 can then again stimulate ERK signalling by binding to EGFR (Epidermal Growth Factor Receptor), suggesting a possible feedback loop. However, it still needs to be determined to what extent the discussed pathways contribute to Piezo1 induced activation of ADAMs.

Notably, effect of the chemical activator Yoda1 on activation of both ADAMs is much stronger than that of mechanical stretch. This may be explained by the sustained activation of all available Piezo1 channels by the chemical activator compared to the spatiotemporal activation of only a few channels localized at the membrane site exposed to mechanical force. Additionally, we observed differences between Yoda1-induced responses when cells were cultured on tissue culture plastic or PDMS substrate. This substrate-dependent variation may be caused by the different involvement of adhesion contacts that are reported to be functionally connected to Piezo1 [53]. Furthermore, increased ADAM shedding activity in response to stretch was only partially supressed by Piezo1 knockdown, while Yoda1-induced shedding activity was completely supressed. This could be due to an incomplete knockdown of about 80 % or could hint to the involvement of other mechanosensing mechanisms. While Piezo1 is probably one of the more relevant mechanoreceptors in lung epithelial cells, these cells do not express the closely related Piezo2 which is predominantly found in neuroexcitable cells [54,55]. However, also other surface molecules play a role for transmitting forces and provoking cellular responses. This may include focal adhesions that contain integrins linking the cells to the

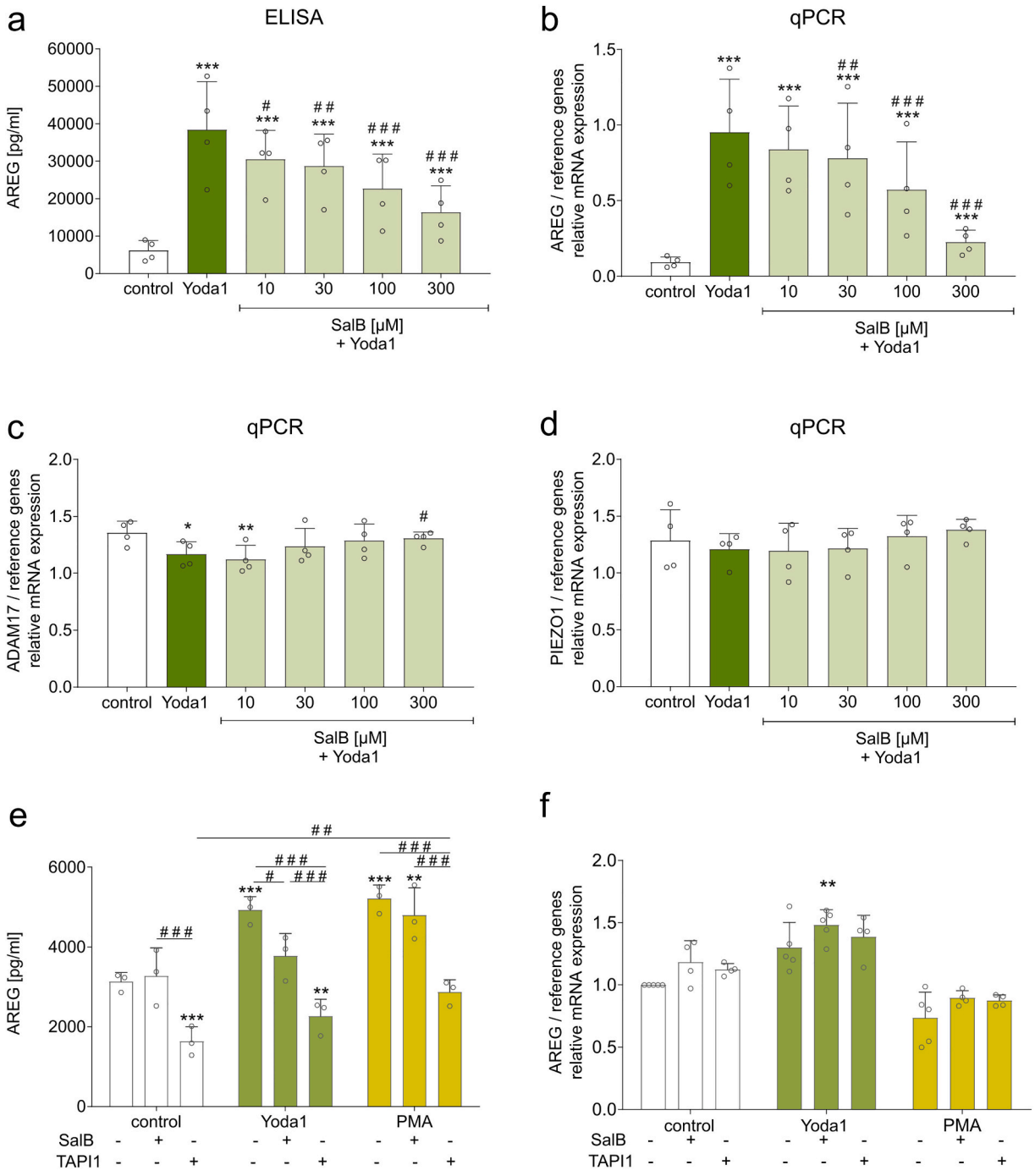

Fig. 6. SalB can inhibit the Yoda1-induced induction and release of AREG in H441 and primary human lung cells. H441 epithelial cells were incubated with the Piezo1 inhibitor SalB at increasing concentrations for 60 min and subsequently stimulated with Yoda1 (10 µM) for 4 h. AREG release was measured via ELISA (a). The relative gene expression of AREG, ADAM17 and Piezo1 was measured via qPCR (b, c, d). Human primary epithelial lung cells were incubated with SalB (300 µM) and TAPI1 (40 µM) or left untreated for 4 h. Subsequently, cells were left unstimulated or stimulated with the indicated concentrations of Yoda1 or PMA. AREG release and gene induction were measured by ELISA (e) and qPCR (f). Quantitative data are shown as mean + SD of at least three independent experiments. Statistical differences to the control without inhibitors are indicated by asterisks (* $p < .05$, ** $p < .01$, *** $p < .001$). In a-d hashes (# $p < .05$, ## $p < .01$, ### $p < .001$) indicate the statistical difference to Yoda1 stimulation and in e-f hashes show the differences between the treatments.

extracellular matrix (ECM). Of note, Piezo1 can be included in this integrin-mediated mechanical stimulation by sensing forces within the cell membrane. Other ion channels such as TRPV4 can also critically contribute to mechanosignalling. However, in our setup TRPV4 does not seem to be of major relevance as indicated by the observation that a TRPV4 agonist failed to induce shedding activity in H441 cells (Suppl. Fig. 16). Although we were able to clearly demonstrate the involvement of Piezo1 with our knockdown experiments, the role of other mechanosensors in stretch-induced ADAM activation needs to be investigated in further experiments.

In addition, we found that Piezo1 stimulation can promote strong mRNA upregulation of AREG but not JAM-A. This was seen for the cell line H441 and also in the ex vivo experiment. Of note, in primary cells such upregulation was not observed. Nevertheless, Piezo1-mediated enhancement of AREG and JAM-A shedding was seen in the cell line as well as in the primary cells and the isolated murine lung. This may

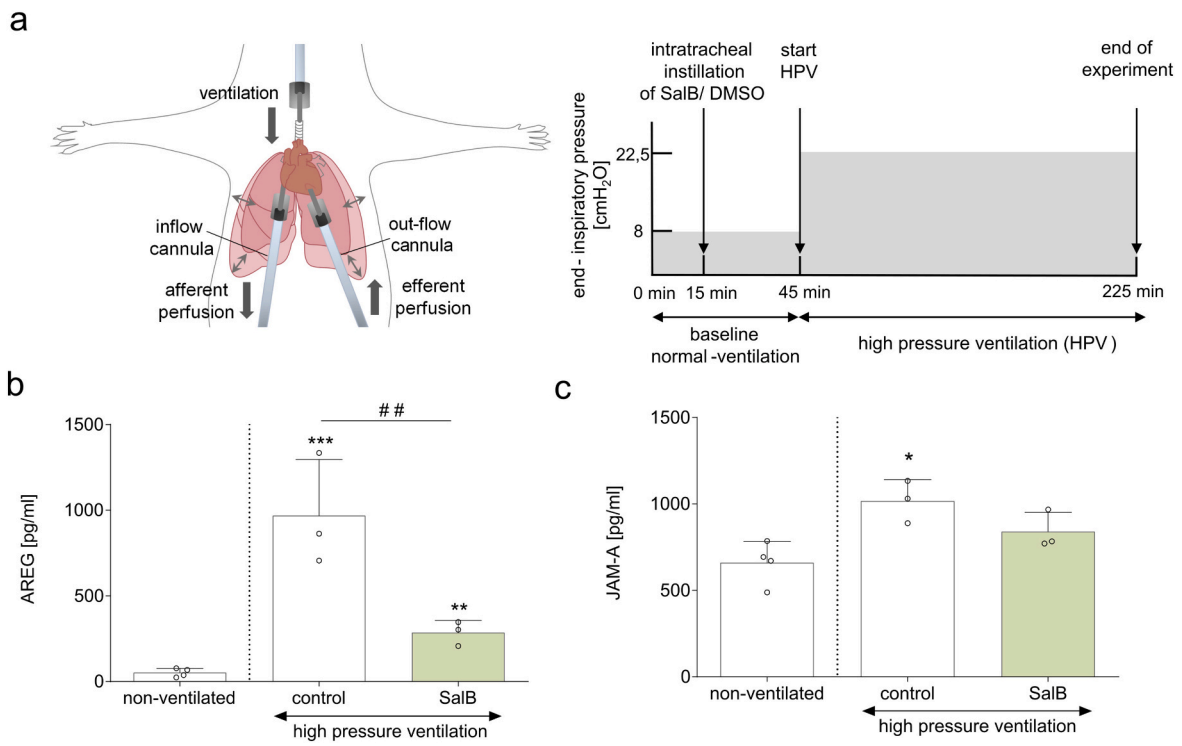

Fig. 7. Increased AREG and JAM-A release in high pressure ventilated murine lungs can be suppressed by Piezo1 inhibition. Isolated perfused lung (IPL) experiments were performed in murine lungs (a). Isolated murine lungs were either treated intratracheally with 50 μl containing SalB (300 μM) or DMSO as control and subsequently ventilated with high pressure. Non-ventilated mice served as controls. Release of AREG (b) and JAM-A (c) into the alveolar space was measured via ELISA of BAL fluids. Quantitative data are shown as mean + SD of at least three independent experiments. Statistical differences to the non-ventilated control are indicated by asterisks (* $p < .05$, ** $p < .01$, *** $p < .001$) and differences between the treatments are indicated by hashes (# $p < .05$, ## $p < .01$, ### $p < .001$).

indicate that the transcriptional effect and the activation of ADAMs are differently regulated and that the different cellular context of the tumour cell line, the primary cells and the multicellular tissue have to be taken into account. Furthermore, for the ex vivo experiment we observed a strong upregulation of AREG mRNA expression which was not suppressed by SalB which may indicate a Piezo1-independent AREG mRNA induction by high pressure ventilation. On the other hand, it is also possible that in the murine lung several cell types besides epithelial cells upregulate AREG mRNA upon high pressure ventilation. These cells may not be sufficiently targeted by the intratracheal application of SalB.

In our study, AREG and JAM-A were identified as natural endogenously expressed epithelial ADAM10 or 17 substrates undergoing regulation by Piezo1. Shedding of AREG has been predominantly reported for ADAM17 [20,56,57]. AREG shedding is already significantly increased after 0.5 h of Yoda1 treatment. However, it is additionally increased after 4 h. This is probably due to the additional upregulation of AREG at the transcriptional level. It is already known that the release of AREG in lung epithelium leads to an activation of EGFR-ERK signalling which in turn induces the de novo synthesis of AREG. This positive feedback loop was linked to a sustained mucus hypersecretion [58]. In primary isolated human lung epithelial cells release of AREG was also increased, but to a lesser extent. Of note, Yoda1-induced mRNA expression of AREG was only slightly but not significantly increased which may explain why no inhibitory effect of SalB on AREG expression could be detected in primary human lung cells. In addition to AREG we also studied JAM-A which is constitutively expressed at lung epithelial cell junctions. We found that Piezo1 signalling does not enhance JAM-A expression but rather stimulates JAM-A release. Previous work from our group has demonstrated that endothelial expressed JAM-A can be shed by ADAM17 and to some degree also by ADAM10 [22]. Since Piezo1 stimulation activates both proteinases in epithelial cells it is conceivable that epithelial JAM-A release involves ADAM17 and ADAM10 as indicated by our pharmacological inhibition experiments. The release of JAM-A was accompanied by a reduced level of JAM-A and E-cadherin in cell junctions. However, the effect was not significant for E-cadherin. This can be explained by the fact that E-cadherin is primarily shed by ADAM10 [40] and Yoda1-mediated ADAM10 activation has a higher EC_{50} than that of ADAM17 in H441 cells.

The Piezo1-induced shedding of growth factors and junction molecules may have considerable consequences for lung epithelial cells. When AREG is released by shedding it will lead to cell stimulation via EGF receptors in an autocrine or paracrine fashion. The signalling of EGFR is required for epithelial regeneration and wound closure [38,59]. However, aberrant signalling can also promote uncontrolled proliferation, apoptosis resistance and cancer. It was already reported that mechanical stretch triggers rapid epithelial cell division via Piezo1 [15]. Our observations suggest that this could be mediated by AREG expression and release via ADAM17. JAM-A and E-cadherin are essential molecules of cell-cell contacts helping to establish the permeability barrier and tight mechanical cohesion. Shedding of JAM-A and E-cadherin by ADAM10 and ADAM17 can promote the disassembly of cell junctions [22,40]. In fact, we observed thinning of JAM-A-stained cell junctions after Piezo1 activation similar to previous work describing reduced adhesion width in VE-cadherin-stained endothelial cell junctions [60]. In the long term, such weakening of tight junctions could increase permeability, which is one of the dysfunctions that can be observed in epithelial tissues experiencing inflammatory or mechanical stress. Additionally, the dissolution of cell contacts would lead to less mechanical cohesion and single cells could then detach from the cell layer. This could be associated with a more migratory and proliferative phenotype. These events have been described as characteristic for epithelial to mesenchymal transition. In fact, ADAM17 has been proposed to play a key role in this process [61]. Our data suggest that such an ADAM17 mediated effect could be in part dependent on mechanical activation which then causes shedding of AREG and adhesion molecules relevant for EMT.

Our ex vivo experiments suggest that Piezo1-mediated ADAM10/17 regulation is relevant in lungs subjected to high pressure ventilation. In patients such ventilation is known to promote acute pulmonary inflammation with severe edema eventually leading to the development of life threatening acute respiratory distress syndrome (ARDS) [62–64]. In this setting, Piezo1 could be an important mechanical activator contributing to the manifestation of this syndrome already at an initial state. It can be envisaged that initially Piezo1-mediated disintegration of cell contacts would lead to edema formation. In fact, opening of cell junctions is a hallmark of ARDS and cyclic stretch of epithelial cells has been reported to enhance protein permeability, which is associated with reduction of junction proteins, disorganization of actin microfilaments, and elevated intracellular calcium concentrations [63,65]. The immediate permeability changes and the tissue injury may be counteracted to some degree by shedding of AREG which has been demonstrated to suppress epithelial cell apoptosis in an experimental model of acute lung injury [66]. AREG expression is considerably upregulated in ARDS. Piezo1-mediated amphiregulin shedding would initially allow repair and healing. However, at a later stage tissue stiffening due to hyperproliferation and fibrosis may be deleterious. In fact, AREG can cause lung fibrosis and stiffening [67]. Eventually, this stiffening might even enhance Piezo1-mediated signalling, since we observed that Yoda1 is a more potent activator of Piezo1-mediated effects on hard substrates than on soft substrates. A similar mechanistic correlation has also been reported for macrophages, that showed attenuated Ca^{2+} influx in response to the Piezo1 agonist Yoda1 with decreasing stiffness and decreased Piezo1 protein expression on soft substrate [68].

Finally, it can be considered whether targeting of Piezo1 in ARDS may represent an option to prevent mechanically induced biotrauma. As a critical proof of concept, orthogonal knockout of Piezo1 could be studied in animal models of ARDS. For therapeutic purpose well characterised pharmacological inhibitors are warranted. Interestingly, the spider venom GsMTx4 was found to alleviate ventilator induced lung injury in rats [69]. However, as with many other described inhibitors of Piezo1, including gadolinium ions also the spider venom GsMTx4 seems to act on other ion channels and may thereby cause unacceptable side effects. Not much is known about the recently described inhibitor SalB that blocks Piezo1 without reported effects on other ion channels [17]. Nevertheless, more studies are needed to scrutinise this compound for its effects on Piezo1 and its usefulness in vivo. We obtained some interesting first results indicating a suppression of Piezo1-mediated shedding events in vitro and ex vivo. However, effects of the compound on lung function remain to be studied in detail and unwanted side effects are possible.

Funding

This work was funded by the Deutsche Forschungsgemeinschaft (DFG, German Research Foundation) – 363055819/GRK2415 and grant Lu869/8-1, by the Bundesministerium für Bildung und Forschung (BMBF) grant 01KI20207, as well as by the START-Program of the Medical Faculty of the RWTH Aachen University, grant 102/22 and the Interdisciplinary Centre for Clinical Research of the Faculty of Medicine of the RWTH Aachen University (OC1-1, OC1-7)

CRediT authorship contribution statement

CG, AP, AH, JS, SH, SB, KB performed experiments and provided data. AL, AB, CM, SD, RM, RL, HJ provided expertise, supervision or critical technique. AL and AB designed the study. CG and AB designed the experiments and designed figs. CG, AB and AH performed statistical analysis. CG, AB and AL wrote the manuscript. All authors critically read and approved the final manuscript.

Declaration of competing interest

The authors declare that they have no known competing financial interests or personal relationships that could have appeared to influence the work reported in this paper.

Data availability

Data will be made available on request.

Acknowledgement

We thank Tanja Woopen for technical assistance. Additionally, we would like to acknowledge and thank Selcan Kahveci-Türköz and Johanna Jakob for her help with experiments and Jens Konrad for his technical expertise and the provided graphics of the stretcher.

Appendix A. Supplementary data

Supplementary data to this article can be found online at https://doi.org/10.1016/j.bioadv.2023.213516.

References

[1] C.M. Waters, E. Roan, D. Navajas, Mechanobiology in Lung Epithelial Cells: Measurements, Perturbations, and Responses, Compr. Physiol., Wiley, 2012, pp. 1–29, https://doi.org/10.1002/cphy.c100090.
[2] D.J. Tschumperlin, F. Boudreault, F. Liu, Recent advances and new opportunities in lung mechanobiology, J. Biomech. 43 (2010) 99–107, https://doi.org/10.1016/j.jbiomech.2009.09.015.
[3] C.D. Cox, N. Bavi, B. Martinac, Biophysical principles of ion-channel-mediated mechanosensory transduction, Cell Rep. 29 (2019) 1–12, https://doi.org/10.1016/j.celrep.2019.08.075.
[4] B. Martinac, C.D. Cox, Mechanosensory transduction: focus on ion channels, in: Ref. Modul. Life Sci, Elsevier, 2017, https://doi.org/10.1016/B978-0-12-809633-8.08094-8.
[5] S.E. Murthy, A.E. Dubin, A. Patapoutian, Piezos thrive under pressure: mechanically activated ion channels in health and disease, Nat. Rev. Mol. Cell Biol. 18 (2017) 771–783, https://doi.org/10.1038/nrm.2017.92.
[6] P. Ridone, M. Vassalli, B. Martinac, Piezo1 mechanosensitive channels: what are they and why are they important, Biophys. Rev. 11 (2019) 795–805, https://doi.org/10.1007/s12551-019-00584-5.
[7] J. Li, B. Hou, S. Tumova, K. Muraki, A. Bruns, M.J. Ludlow, A. Sedo, A.J. Hyman, L. McKeown, R.S. Young, N.Y. Yuldasheva, Y. Majeed, L.A. Wilson, B. Rode, M. A. Bailey, H.R. Kim, Z. Fu, D.A.L. Carter, J. Bilton, H. Imrie, P. Ajuh, T.N. Dear, R. M. Cubbon, M.T. Kearney, K.R. Prasad, P.C. Evans, J.F.X. Ainscough, D.J. Beech, Piezo1 integration of vascular architecture with physiological force, Nature 515 (2014) 279–282, https://doi.org/10.1038/nature13701.
[8] S.S. Ranade, Z. Qiu, S.H. Woo, S.S. Hur, S.E. Murthy, S.M. Cahalan, J. Xu, J. Mathur, M. Bandell, B. Coste, Y.S.J. Li, S. Chien, A. Patapoutian, Piezo1, a mechanically activated ion channel, is required for vascular development in mice, Proc. Natl. Acad. Sci. U. S. A. 111 (2014) 10347–10352, https://doi.org/10.1073/pnas.1409233111.
[9] S.P. Wang, R. Chennupati, H. Kaur, A. Iring, N. Wettschureck, S. Offermanns, Endothelial cation channel PIEZO1 controls blood pressure by mediating flow-induced ATP release, J. Clin. Invest. 126 (2016) 4527–4536, https://doi.org/10.1172/JCI87343.
[10] S.M. Cahalan, V. Lukacs, S.S. Ranade, S. Chien, M. Bandell, A. Patapoutian, Piezo1 links mechanical forces to red blood cell volume, Elife. 4 (2015), https://doi.org/10.7554/eLife.07370.
[11] S. Wang, B. Wang, Y. Shi, T. Möller, R.I. Stegmeyer, B. Strilic, T. Li, Z. Yuan, C. Wang, N. Wettschureck, D. Vestweber, S. Offermanns, Mechanosensation by endothelial PIEZO1 is required for leukocyte diapedesis, Blood. 140 (2022) 171–183, https://doi.org/10.1182/blood.2021014614.
[12] G.T. Eisenhoffer, P.D. Loftus, M. Yoshigi, H. Otsuna, C.-B. Chien, P.A. Morcos, J. Rosenblatt, Crowding induces live cell extrusion to maintain homeostatic cell numbers in epithelia, Nature. 484 (2012) 546–549, https://doi.org/10.1038/nature10999.
[13] Y. Zhang, L. Jiang, T. Huang, D. Lu, Y. Song, L. Wang, J. Gao, Mechanosensitive cation channel Piezo1 contributes to ventilator-induced lung injury by activating RhoA/ROCK1 in rats, Respir. Res. 22 (2021) 1–14, https://doi.org/10.1186/s12931-021-01844-3.
[14] K. Diem, M. Fauler, G. Fois, A. Hellmann, N. Winokurow, S. Schumacher, C. Kranz, M. Frick, Mechanical stretch activates piezo1 in caveolae of alveolar type I cells to trigger ATP release and paracrine stimulation of surfactant secretion from alveolar type II cells, FASEB J. 34 (2020) 12785–12804, https://doi.org/10.1096/fj.202000613RRR.
[15] S. Gudipaty, J. Lindblom, P. Loftus, M. Redd, K. Edes, C. Davey, V. Krishnegowda, J. Rosenblatt, Mechanical stretch triggers rapid epithelial cell division through

Piezo1, Nature. 543 (2017) 118–121, https://doi.org/10.1038/nature21407. Mechanical.
[16] R. Syeda, J. Xu, A.E. Dubin, B. Coste, J. Mathur, T. Huynh, J. Matzen, J. Lao, D. C. Tully, I.H. Engels, H. Michael Petrassi, A.M. Schumacher, M. Montal, M. Bandell, A. Patapoutian, Chemical activation of the mechanotransduction channel Piezo1, Elife. 4 (2015) 1–11, https://doi.org/10.7554/eLife.07369.
[17] X. Pan, R. Wan, Y. Wang, S. Liu, Y. He, B. Deng, S. Luo, Y. Chen, L. Wen, T. Hong, H. Xu, Y. Bian, M. Xia, J. Li, Inhibition of chemically and mechanically activated Piezo1 channels as a mechanism for ameliorating atherosclerosis with salvianolic acid B, Br. J. Pharmacol. 179 (2022) 3778–3814, https://doi.org/10.1111/bph.15826.
[18] J. Pruessmeyer, A. Ludwig, The good, the bad and the ugly substrates for ADAM10 and ADAM17 in brain pathology, inflammation and cancer, Semin. Cell Dev. Biol. 20 (2009) 164–174, https://doi.org/10.1016/j.semcdb.2008.09.005.
[19] B.N. Lambrecht, M. Vanderkerken, H. Hammad, The emerging role of ADAM metalloproteinases in immunity, Nat. Rev. Immunol. 18 (2018) 745–758, https://doi.org/10.1038/s41577-018-0068-5.
[20] U. Sahin, G. Weskamp, K. Kelly, H.-M. Zhou, S. Higashiyama, J. Peschon, D. Hartmann, P. Saftig, C.P. Blobel, Distinct roles for ADAM10 and ADAM17 in ectodomain shedding of six EGFR ligands, J. Cell Biol. 164 (2004) 769–779, https://doi.org/10.1083/jcb.200307137.
[21] R.A. Black, C.T. Rauch, C.J. Kozlosky, J.J. Peschon, J.L. Slack, M.F. Wolfson, B. J. Castner, K.L. Stocking, P. Reddy, S. Srinivasan, N. Nelson, N. Boiani, K. A. Schooley, M. Gerhart, R. Davis, J.N. Fitzner, R.S. Johnson, R.J. Paxton, C. J. March, D.P. Cerretti, A metalloproteinase disintegrin that releases tumour-necrosis factor-α from cells, Nature. 385 (1997) 729–733, https://doi.org/10.1038/385729a0.
[22] R.R. Koenen, J. Pruessmeyer, O. Soehnlein, L. Fraemohs, A. Zernecke, N. Schwarz, K. Reiss, A. Sarabi, L. Lindbom, T.M. Hackeng, C. Weber, A. Ludwig, Regulated release and functional modulation of junctional adhesion molecule A by disintegrin metalloproteinases, Blood. 113 (2009) 4799–4809, https://doi.org/10.1182/blood-2008-04-152330.
[23] S. Düsterhöft, A. Babendreyer, A.A. Giese, C. Flasshove, A. Ludwig, Status update on iRhom and ADAM17: It's still complicated, Biochim. Biophys. Acta Mol. Cell Res. 2019 (1866) 1567–1583, https://doi.org/10.1016/j.bbamcr.2019.06.017.
[24] C. Hundhausen, D. Misztela, T.A. Berkhout, N. Broadway, P. Saftig, K. Reiss, D. Hartmann, F. Fahrenholz, R. Postina, V. Matthews, K.-J. Kallen, S. Rose-John, A. Ludwig, The disintegrin-like metalloproteinase ADAM10 is involved in constitutive cleavage of CX3CL1 (fractalkine) and regulates CX3CL1-mediated cell-cell adhesion, Blood. 102 (2003) 1186–1195, https://doi.org/10.1182/blood-2002-12-3775.
[25] C. Hundhausen, A. Schulte, B. Schulz, M.G. Andrzejewski, N. Schwarz, P. von Hundelshausen, U. Winter, K. Paliga, K. Reiss, P. Saftig, C. Weber, A. Ludwig, Regulated shedding of transmembrane chemokines by the Disintegrin and metalloproteinase 10 facilitates detachment of adherent leukocytes, J. Immunol. 178 (2007) 8064–8072, https://doi.org/10.4049/jimmunol.178.12.8064.
[26] V. Caolo, M. Debant, N. Endesh, T.S. Futers, L. Lichtenstein, F. Bartoli, G. Parsonage, E.A.V. Jones, D.J. Beech, Shear stress activates ADAM10 sheddase to regulate Notch1 via the Piezo1 force sensor in endothelial cells, Elife. 9 (2020) 1–18, https://doi.org/10.7554/eLife.50684.
[27] A.D. Rieg, N.A. Bünting, C. Cranen, S. Suleiman, J.W. Spillner, H. Schnöring, T. Schröder, S. von Stillfried, T. Braunschweig, P.W. Manley, G. Schälte, R. Rossaint, S. Uhlig, C. Martin, Tyrosine kinase inhibitors relax pulmonary arteries in human and murine precision-cut lung slices, Respir. Res. 20 (2019) 111, https://doi.org/10.1186/s12931-019-1074-2.
[28] A. Babendreyer, L. Molls, I.M. Simons, D. Dreymueller, K. Biller, H. Jahr, B. Denecke, R.A. Boon, S. Bette, U. Schnakenberg, A. Ludwig, The metalloproteinase ADAM15 is upregulated by shear stress and promotes survival of endothelial cells, J. Mol. Cell. Cardiol. 134 (2019) 51–61, https://doi.org/10.1016/j.yjmcc.2019.06.017.
[29] J.M. Ruijter, C. Ramakers, W.M.H. Hoogaars, Y. Karlen, O. Bakker, M.J.B. van den Hoff, A.F.M. Moorman, Amplification efficiency: linking baseline and bias in the analysis of quantitative PCR data, Nucleic Acids Res. 37 (2009) e45, https://doi.org/10.1093/nar/gkp045.
[30] R. Püllen, J. Konrad, B. Hoffmann, R. Merkel, Mechanobiology Methods and Protocols (Methods in Molecular Biology), MIMB, Volu, Springer, 2023.
[31] U. Faust, N. Hampe, W. Rubner, N. Kirchgeßner, S. Safran, B. Hoffmann, R. Merkel, Cyclic stress at mHz frequencies aligns fibroblasts in direction of zero strain, PLoS One 6 (2011), e28963, https://doi.org/10.1371/journal.pone.0028963.
[32] Y. Kubo, B. Hoffmann, K. Goltz, U. Schnakenberg, H. Jahr, R. Merkel, G. Schulze-Tanzil, T. Pufe, M. Tohidnezhad, Different frequency of cyclic tensile strain relates to anabolic/catabolic conditions consistent with Immunohistochemical staining intensity in tenocytes, Int. J. Mol. Sci. 21 (2020) 1082, https://doi.org/10.3390/ijms21031082.
[33] H.-D. Held, C. Martin, S. Uhlig, Characterization of airway and vascular responses in murine lungs, Br. J. Pharmacol. 126 (1999) 1191–1199, https://doi.org/10.1038/sj.bjp.0702394.
[34] J. Krabbe, N. Ruske, T. Braunschweig, S. Kintsler, J.W. Spillner, T. Schröder, S. Kalverkamp, S. Kanzler, A.D. Rieg, S. Uhlig, C. Martin, The effects of hydroxyethyl starch and gelatine on pulmonary cytokine production and oedema formation, Sci. Rep. 8 (2018) 5123, https://doi.org/10.1038/s41598-018-23513-0.
[35] H. Liu, J. Hu, Q. Zheng, X. Feng, F. Zhan, X. Wang, G. Xu, F. Hua, Piezo1 channels as force sensors in mechanical force-related chronic inflammation, Front. Immunol. 13 (2022) 1–20, https://doi.org/10.3389/fimmu.2022.816149.
[36] A. Ludwig, C. Hundhausen, M. Lambert, N. Broadway, R. Andrews, D. Bickett, M. Leesnitzer, J. Becherer, Metalloproteinase inhibitors for the Disintegrin-like metalloproteinases ADAM10 and ADAM17 that differentially block constitutive and Phorbol Ester-inducible shedding of cell surface molecules, Comb. Chem. High Throughput Screen. 8 (2005) 161–171, https://doi.org/10.2174/1386207053258488.
[37] D.M.W. Zaiss, W.C. Gause, L.C. Osborne, D. Artis, Emerging functions of Amphiregulin in orchestrating immunity, inflammation, and tissue repair, Immunity. 42 (2015) 216–226, https://doi.org/10.1016/j.immuni.2015.01.020.
[38] S.S. Singh, S.B. Chauhan, A. Kumar, S. Kumar, C.R. Engwerda, S. Sundar, R. Kumar, Amphiregulin in cellular physiology, health, and disease: potential use as a biomarker and therapeutic target, J. Cell. Physiol. 237 (2022) 1143–1156, https://doi.org/10.1002/jcp.30615.
[39] J.W. Brooks, R.G. Parton, A.S. Yap, K. Duszyc, Epithelial mechanosensing at cell-cell contacts and tight junctions, in: Tight Junctions, Springer International Publishing, Cham, 2022, pp. 27–50, https://doi.org/10.1007/978-3-030-97204-2_3.
[40] T. Maretzky, K. Reiss, A. Ludwig, J. Buchholz, F. Scholz, E. Proksch, B. de Strooper, D. Hartmann, P. Saftig, ADAM10 mediates E-cadherin shedding and regulates epithelial cell-cell adhesion, migration, and β-catenin translocation, Proc. Natl. Acad. Sci. 102 (2005) 9182–9187, https://doi.org/10.1073/pnas.0500918102.
[41] M. Zhong, W. Wu, H. Kang, Z. Hong, S. Xiong, X. Gao, J. Rehman, Y.A. Komarova, A.B. Malik, Alveolar stretch activation of endothelial Piezo1 protects Adherens junctions and lung vascular barrier, Am. J. Respir. Cell Mol. Biol. 62 (2020) 168–177, https://doi.org/10.1165/rcmb.2019-0024OC.
[42] L.K. Reiss, A. Schuppert, S. Uhlig, Inflammatory processes during acute respiratory distress syndrome, Curr. Opin. Crit. Care 24 (2018) 1–9, https://doi.org/10.1097/MCC.0000000000000472.
[43] L.K. Reiss, A. Fragoulis, S. Siegl, C. Platen, Y.W. Kan, J. Nautiyal, M. Parker, T. Pufe, U. Uhlig, C. Martin, S. Uhlig, C.J. Wruck, Interplay between nuclear factor erythroid 2–related factor 2 and Amphiregulin during mechanical ventilation, Am. J. Respir. Cell Mol. Biol. 51 (2014) 668–677, https://doi.org/10.1165/rcmb.2013-0279OC.
[44] J. Suzuki, T. Fujii, T. Imao, K. Ishihara, H. Kuba, S. Nagata, Calcium-dependent phospholipid scramblase activity of TMEM16 protein family members, J. Biol. Chem. 288 (2013) 13305–13316, https://doi.org/10.1074/jbc.M113.457937.
[45] M. Veit, K.I. Koyro, B. Ahrens, F. Bleibaum, M. Munz, H. Rövekamp, J. Andrä, R. Schreiber, K. Kunzelmann, A. Sommer, S. Bhakdi, K. Reiss, Anoctamin-6 regulates ADAM sheddase function, Biochim. Biophys. Acta Mol. Cell Res. 2018 (1865) 1598–1610, https://doi.org/10.1016/j.bbamcr.2018.08.011.
[46] A. Sommer, F. Kordowski, J. Büch, T. Maretzky, A. Evers, J. Andrä, S. Düsterhöft, M. Michalek, I. Lorenzen, P. Somasundaram, A. Tholey, F.D. Sönnichsen, K. Kunzelmann, L. Heinbockel, C. Nehls, T. Gutsmann, J. Grötzinger, S. Bhakdi, K. Reiss, Phosphatidylserine exposure is required for ADAM17 sheddase function, Nat. Commun. 7 (2016) 11523, https://doi.org/10.1038/ncomms11523.
[47] S. Düsterhöft, M. Michalek, F. Kordowski, M. Oldefest, A. Sommer, J. Röseler, K. Reiss, J. Grötzinger, I. Lorenzen, Extracellular Juxtamembrane segment of ADAM17 interacts with membranes and is essential for its shedding activity, Biochemistry. 54 (2015) 5791–5801, https://doi.org/10.1021/acs.biochem.5b00497.
[48] M. Cavadas, I. Oikonomidi, C.J. Gaspar, E. Burbridge, M. Badenes, I. Félix, A. Bolado, T. Hu, A. Bileck, C. Gerner, P.M. Domingos, A. von Kriegsheim, C. Adrain, Phosphorylation of iRhom2 controls stimulated proteolytic shedding by the metalloprotease ADAM17/TACE, Cell Rep. 21 (2017) 745–757, https://doi.org/10.1016/j.celrep.2017.09.074.
[49] A. Babendreyer, D.M. Rojas-González, A.A. Giese, S. Fellendorf, S. Düsterhöft, P. Mela, A. Ludwig, Differential induction of the ADAM17 regulators iRhom1 and 2 in endothelial cells, Front. Cardiovasc. Med. 7 (2020), https://doi.org/10.3389/fcvm.2020.610344.
[50] A. Sommer, A. Fries, I. Cornelsen, N. Speck, F. Koch-Nolte, G. Gimpl, J. Andrä, S. Bhakdi, K. Reiss, Melittin modulates keratinocyte function through P2 receptor-dependent ADAM activation, J. Biol. Chem. 287 (2012) 23678–23689, https://doi.org/10.1074/jbc.M112.362756.
[51] N.G. dela Paz, J.A. Frangos, Yoda1-induced phosphorylation of Akt and ERK1/2 does not require Piezo1 activation, Biochem. Biophys. Res. Commun. 497 (2018) 220–225, https://doi.org/10.1016/j.bbrc.2018.02.058.
[52] L.G. Navar, M. Gooz, H.L. Bell, M. Göoz, ADAM-17 is activated by the Mitogenic protein kinase ERK in a model of kidney fibrosis, Am J Med Sci 339 (2010) 105–107, https://doi.org/10.1097/MAJ.0b013e3181cb4487.
[53] X. Chen, S. Wanggou, A. Bodalia, M. Zhu, W. Dong, J.J. Fan, W.C. Yin, H.-K. Min, M. Hu, D. Draghici, W. Dou, F. Li, F.J. Coutinho, H. Whetstone, M.M. Kushida, P. B. Dirks, Y. Song, C. Hui, Y. Sun, L.-Y. Wang, X. Li, X. Huang, A feedforward mechanism mediated by mechanosensitive ion channel PIEZO1 and tissue mechanics promotes glioma aggression, Neuron. 100 (2018) 799–815.e7, https://doi.org/10.1016/j.neuron.2018.09.046.
[54] B. Xiao, Levering mechanically activated piezo channels for potential pharmacological intervention, Annu. Rev. Pharmacol. Toxicol. 60 (2020) 195–218, https://doi.org/10.1146/annurev-pharmtox-010919-023703.
[55] J. Wu, A.H. Lewis, J. Grandl, Touch, tension, and transduction – the function and regulation of piezo ion channels, Trends Biochem. Sci. 42 (2017) 57–71, https://doi.org/10.1016/j.tibs.2016.09.004.
[56] C.L. Hinkle, S.W. Sunnarborg, D. Loiselle, C.E. Parker, M. Stevenson, W.E. Russell, D.C. Lee, Selective roles for tumor necrosis factor α-converting enzyme/ADAM17 in the shedding of the epidermal growth factor receptor ligand family. The juxtamembrane stalk determines cleavage efficiency, J. Biol. Chem. 279 (2004) 24179–24188, https://doi.org/10.1074/jbc.M312141200.

[57] S.W. Sunnarborg, C.L. Hinkle, M. Stevenson, W.E. Russell, C.S. Raska, J.J. Peschon, B.J. Castner, M.J. Gerhart, R.J. Paxton, R.A. Black, D.C. Lee, Tumor necrosis factor-α converting enzyme (TACE) regulates epidermal growth factor receptor ligand availability, J. Biol. Chem. 277 (2002) 12838–12845, https://doi.org/10.1074/jbc.M112050200.
[58] L. Huang, J. Pu, F. He, B. Liao, B. Hao, W. Hong, X. Ye, J. Chen, J. Zhao, S. Liu, J. Xu, B. Li, P. Ran, Positive feedback of the amphiregulin-EGFR-ERK pathway mediates PM2.5 from wood smoke-induced MUC5AC expression in epithelial cells, Sci. Rep. 7 (2017) 11084, https://doi.org/10.1038/s41598-017-11541-1.
[59] C. Berasain, M.A. Avila, Amphiregulin, Semin. Cell Dev. Biol. 28 (2014) 31–41, https://doi.org/10.1016/j.semcdb.2014.01.005.
[60] E.E. Friedrich, Z. Hong, S. Xiong, M. Zhong, A. Di, J. Rehman, Y.A. Komarova, A. B. Malik, Endothelial cell Piezo1 mediates pressure-induced lung vascular hyperpermeability via disruption of adherens junctions, Proc. Natl. Acad. Sci. U. S. A. 116 (2019) 12980–12985, https://doi.org/10.1073/pnas.1902165116.
[61] M. Sisto, D. Ribatti, S. Lisi, ADAM 17 and epithelial-to-mesenchymal transition: the evolving story and its link to fibrosis and Cancer, J. Clin. Med. 10 (2021) 3373, https://doi.org/10.3390/jcm10153373.
[62] R. Herrero, G. Sanchez, J.A. Lorente, New insights into the mechanisms of pulmonary edema in acute lung injury, Ann. Transl. Med. 6 (2018) 32, https://doi.org/10.21037/atm.2017.12.18.
[63] K.J. Cavanaugh, J. Oswari, S.S. Margulies, Role of stretch on tight junction structure in alveolar epithelial cells, Am. J. Respir. Cell Mol. Biol. 25 (2001) 584–591, https://doi.org/10.1165/ajrcmb.25.5.4486.
[64] A. Serpa Neto, S.O. Cardoso, J.A. Manetta, V.G.M. Pereira, D.C. Espósito, M. de O. P. Pasqualucci, M.C.T. Damasceno, M.J. Schultz, Association between use of lung-protective ventilation with lower tidal volumes and clinical outcomes among patients without acute respiratory distress syndrome, JAMA. 308 (2012) 1651, https://doi.org/10.1001/jama.2012.13730.
[65] K.J. Cavanaugh, T.S. Cohen, S.S. Margulies, Stretch increases alveolar epithelial permeability to uncharged micromolecules, Am. J. Physiol. Physiol. 290 (2006) C1179–C1188, https://doi.org/10.1152/ajpcell.00355.2004.
[66] S. Ogata-Suetsugu, T. Yanagihara, N. Hamada, C. Ikeda-Harada, T. Yokoyama, K. Suzuki, T. Kawaguchi, T. Maeyama, K. Kuwano, Y. Nakanishi, Amphiregulin suppresses epithelial cell apoptosis in lipopolysaccharide-induced lung injury in mice, Biochem. Biophys. Res. Commun. 484 (2017) 422–428, https://doi.org/10.1016/j.bbrc.2017.01.142.
[67] L. Ding, T. Liu, Z. Wu, B. Hu, T. Nakashima, M. Ullenbruch, F. Gonzalez De Los Santos, S.H. Phan, Bone marrow CD11c + cell–derived amphiregulin promotes pulmonary fibrosis, J. Immunol. 197 (2016) 303–312, https://doi.org/10.4049/jimmunol.1502479.
[68] H. Atcha, A. Jairaman, J.R. Holt, V.S. Meli, R.R. Nagalla, P.K. Veerasubramanian, K.T. Brumm, H.E. Lim, S. Othy, M.D. Cahalan, M.M. Pathak, W.F. Liu, Mechanically activated ion channel Piezo1 modulates macrophage polarization and stiffness sensing, Nat. Commun. 12 (2021), https://doi.org/10.1038/s41467-021-23482-5.
[69] Y. Zhang, L. Jiang, T. Huang, D. Lu, Y. Song, L. Wang, J. Gao, Mechanosensitive cation channel Piezo1 contributes to ventilator-induced lung injury by activating RhoA/ROCK1 in rats, Respir. Res. 22 (2021) 250, https://doi.org/10.1186/s12931-021-01844-3.

Caroline Grannemann received her B.Sc. and M. Sc. degree in biology from RWTH Aachen University, Germany. During her studies she worked in research projects at Stockholm University, Sweden and Cambridge University, England. The study of this article forms part of her doctoral degree about mechanobiology in epithelial cells, focusing on the Piezo1/ ADAM axis, at the Institute of Pharmacology and Toxicology at University Hospital RWTH Aachen. Her project is part of the graduate school ME3T (Mechanobiology in Epithelial 3D Tissue Constructs).

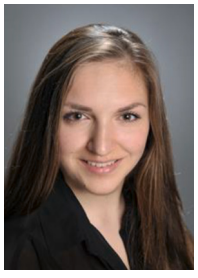

Alessa Pabst received her B.Sc. in Biotechnology at the University of Applied Science Aachen, Germany, in 2018 and her M.Sc. in Molecular and Applied Biotechnology at the RWTH Aachen University in 2021. At the Institute of Molecular Pharmacology at the University Hospital RWTH Aachen she started her research in the field of Mechanobiology in 2020. Since 2022, she is a PhD candidate in association with the graduate school ME3T (Mechanobiology in Epithelial 3D Tissue Constructs) and investigates in this context, how mechanical stimuli activate ADAM proteases via mechanosensitive ion channels in primary endothelial cells.

Annika Honert received the B. Sc. in biology from the RWTH Aachen University, Germany and won the Schöneborn price 2019 for her outstanding achievements during her studies. For her master's degree she specialized into the field of medical life science and is currently writing her master thesis on inflammation regulation in the lung at the Institute of Pharmacology and Toxicology at University Hospital RWTH Aachen in the group of Prof. Andreas Ludwig. Since 2020 she works as a scientific assistant at the Institute of Pathology at University Hospital RWTH Aachen in the group of Prof. Dahl.

Jana Schieren studied Biomedical Engineering at the University of Applied Sciences Aachen and received her B.Eng. and M. Sc. degrees in 2017 and 2019. Currently, she investigates the role of keratin intermediate filaments in force homeostasis of epidermal tissue at the Institute for Molecular and Cellular Anatomy of the RWTH Aachen University. In the context of this work, she pursues her doctorate degree in association with the graduate school ME3T (Mechanobiology in Epithelial 3D Tissue Constructs).

Christian Martin studied chemistry at the University of Tuebingen. He then obtained his doctorate in biochemical pharmacology at the University of Constance. He currently heads the Institute of Pharmacology and Toxicology at RWTH Aachen University.

Sophia Hank has been studying medicine at RWTH Aachen University since 2016. She passed her first state examination in 2019, her second in 2022 and became a scholarship holder of the doctoral programme of the medical faculty in 2020. For her doctoral thesis, she has been conducting research at the Institute of Pharmacology and Toxicology at RWTH Aachen University in Prof. Martin's lung pharmacology group since 2021, where a large component of her research is the Isolated Perfused Lung (IPL) model.

Svenja Böll received her B. Sc. in Forensic Science at Bonn-Rhein-Sieg University of Applied Sciences in 2011. This was followed in 2013 by her M. Sc. in toxicology at Heinrich Heine University in Düsseldorf. She graduated with her dissertation on the topic of the effect of acid sphingomyelinase in allergic T_H2-directed bronchial asthma in 2021 at RWTH Aachen University. She then continued her research on this topic as a postdoc until 2022.

Katharina Bläsius studied biology at the RWTH Aachen University, Germany. She received her B. Sc. in 2018 and her M. Sc. in 2021. In 2020, she started her research at the Institute of Molecular Pharmacology at University Hospital RWTH Aachen with a focus on novel interaction partners of iRhom pseudoproteases. Her PhD is funded by the RWTH doctoral scholarship (RWTH-Graduiertenförderung).

Stefan Düsterhöft studied Biochemistry and Molecular Biology at Kiel University, Germany and received his Diploma degree in 2010. He started his research in the field of molecular and structural biology of ectodomain shedding at the Institute of Biochemistry at Kiel University in the group of Prof. Joachim Grötzinger. In 2014, he received his doctorate degree (rer. nat.). From 2015 to 2017, he received a DFG fellowship to work as postdoc at the Sir William Dunn School of Pathology at the University of Oxford in the group of Prof. Matthew Freeman. Since 2017 he is head of the research group "Molecular Biology of Signalling in Inflammatory Processes" at the Institute of Molecular Pharmacology at University Hospital RWTH Aachen.

Holger Jahr graduated in Microbiology and Gene Technology at, and received his PhD in Biology from, the former German Excellence University in Bielefeld. After post-doc periods in Groningen and at Stanford University Medical Center, he spent 12 years working for the Erasmus MC University Medical Center (Depts. of Internal Medicine and Orthopaedics). In 2013, he joined the University Hospital of the RWTH Aachen. As a trained anatomist and Associate Professor of Anatomy and Experimental Orthopaedics, he is currently heading the Biomaterials and Molecular Musculoskeletal Research at the Dept. of Anatomy and Cell Biology in Aachen.

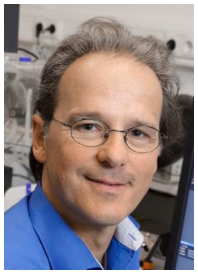

Rudolf Merkel studied general physics at the Technical University Munich, Germany, and received his Dipl.-Phys degree in 1988. After he received his Ph.D. from the same university in 1993, he went to the University of British Columbia (Vancouver, BC, Canada) were he stayed as postdoc for two years. Subsequently, he returned to Munich as leader of an independent junior research group. He was appointed as director of an institute at the Forschungszentrum Jülich, Germany, in 2001 and one year later as full professor in Physical Chemistry at Bonn University, Germany.

Rudolf Leube studied chemical engineering and medicine in St. Louis, Tübingen and Marburg. He spent his postgraduate time at the German Cancer Research Centre in Heidelberg and was appointed as professor of anatomy at Mainz University in 1996. In 2008 he moved to RWTH Aachen University to head the Institute of Molecular and Cellular Anatomy. Rudolf Leube is currently acting as spokesperson of the graduate school "Mechanobiology in Epithelial 3D Tissue Constructs".

Aaron Babendreyer studied biology at the RWTH Aachen University, Germany, and received his M. Sci. degree in 2012. He started his research in the field of mechanobiology at the Institute of Pharmacology and Toxicology at University Hospital RWTH Aachen in the group of Prof. Andreas Ludwig. In 2018, he received his doctorate degree (rer. nat.). Since 2018, he is head of the research group "Vascular Mechanobiology and Inflammation" at the Institute of Molecular Pharmacology at University Hospital RWTH Aachen. In 2022, he received his master's degree in the Medical Data Science master's program at the RWTH International Academy Aachen.

Andreas Ludwig studied biology at the University of Kiel, Germany. He is the director of the Institute of Molecular Pharmacology at the RWTH Aachen University, Germany. A major focus of his research is on the regulation and activity of ADAM-family metalloproteinase in inflammatory diseases. A recent research project investigates how mechanical forces modulate the inflammatory response of endothelial and epithelial cells.